NASA Technical Memorandum 4521

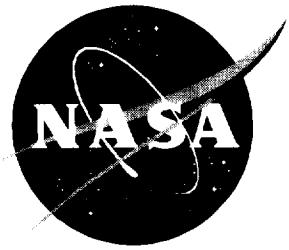

Techniques To Improve Maneuver Stability Characteristics of a Nonlinear Wide-Body Transport Airplane in Cruise Flight

William D. Grantham and Lee H. Person, Jr.
Langley Research Center • Hampton, Virginia

Melvin L. Bailey
Lockheed Engineering & Sciences Company • Hampton, Virginia

Stephen A. Tingas
Lockheed Aeronautical Systems Company • Marietta, Georgia

National Aeronautics and Space Administration
Langley Research Center • Hampton, Virginia 23681-0001

March 1994

Summary

NASA, the Federal Aviation Administration, and the Lockheed Corporation performed a cooperative flight simulation experiment in the six-degree-of-freedom, ground-based, Langley Visual/Motion Simulator (VMS). An objective of the study was to provide engineering guidance for acceptable nonlinear maneuver stability characteristics for transport aircraft. The baseline mathematical model of the airplane represented a wide-body jet transport with a pitch active control system (PACS). The PACS is a simulation of an experimental pitch-rate damper that is installed on a single Lockheed L-1011 aircraft used for in-flight research. The PACS provided acceptable flying qualities for negative static margins to 5 percent. As the aircraft center of gravity moved aft and the static margin changed from positive to negative, the maneuver stability characteristics were modified through systematic variations of PACS, pitch-rate damper gain, control loading (column force per column deflection (F_c/δ_c)), and control gearing (horizontal-tail deflection per control force (δ_H/δ_c)). The evaluation tasks consisted of performing (1) small pitch-attitude changes, (2) standard operational turns, and (3) wind-up turns at an altitude of 33 000 ft at a Mach number of 0.83, and in calm atmospheric conditions. Nonlinear maneuver stability is defined as a nonincremental change in stick force required to effect an incremental change in normal acceleration.

The results of this experiment verify current military specification boundaries for linear maneuver stability characteristics. Also for linear maneuver stability cases, a degradation in pilot ratings at extreme values of column force per normal acceleration (F_c/n_z) was evident for all tasks performed with the statically unstable configurations. However, statically stable configurations appeared to be degraded only in high-load-factor tasks (i.e., wind-up turns). The maneuver stability was made linear by either adjusting F_c/δ_c or δ_H/δ_c. The results indicate that variations in δ_H/δ_c, as opposed to F_c/δ_c, to maintain linear F_c/n_z provide improved flying qualities in the upper F_c/n_z range, but provide no advantage in the lower range. However, these two parameters are definitely coupled; that is, an acceptable range of δ_H/δ_c at a fixed value of F_c/δ_c may not be acceptable at another value of F_c/δ_c.

The results indicate that for the nonlinear maneuver stability cases evaluated, substantial levels of nonlinearity are acceptable to the pilots as long as actual column force at selected load factors remains within the current military specifications for level 1 (satisfactory) extremes (23.3 lbf/g and 80 lbf/g). Pilot ratings were acquired for F_c/n_z variations with a single break at $n_z = 1.333g$ or $1.667g$ and with an initial slope of 50 lbf/g. As expected, pilots preferred an increase, not a reduction, in the slope of high load factors when the break occurred at $n_z = 1.333g$. Slope reduction was more noticeable to the pilots than slope increase. A comparison of the two methods used to control the maneuver stability characteristics shows little difference in the break at $1.333g$. However, with the break at $1.667g$, pilots preferred a fixed δ_H/δ_c, with variable F_c/δ_c, particularly for higher F_c/n_z slopes. This comparison provides insight into a possible means of linearizing the maneuver stability characteristics of a control system with inherent nonlinearities.

Introduction

The longitudinal maneuver control force gradient in an aircraft is a critical parameter of flying qualities that ensures structural protection as well as adequate prediction of load-factor control for the pilot. Currently, maneuver stability flight characteristics are not uniquely addressed in Federal Aviation Regulations (FAR) Part 25 for transport aircraft (ref. 1). In previous transport category certification programs, the Federal Aviation Administration (FAA) used a combination of requirements (longitudinal control, vibration and buffeting, high-speed characteristics, and out-of-trim characteristics) to ensure safe and controllable maneuver stability characteristics over a range of flight conditions and aircraft configurations. These regulations are controversial and require a considerable amount of time for design studies and tests (ref. 2). Additional engineering guidance is needed to identify acceptable nonlinear maneuver stability characteristics, particularly for relaxed stability, highly augmented transport configurations. The current trend in large aircraft design, such as the Airbus A320 (ref. 3), is toward relaxed, or even negative, static margins for improved fuel efficiency. Advanced flight control systems developed for these aircraft, in many instances, have rendered current maneuver stability criteria either too stringent or of little practical use.

Swept-wing high-subsonic aircraft are prone to exhibiting nonlinear maneuver stability characteristics at higher load factors. Figure 1 shows the amount of column force (F_c) required by the simulated aircraft to command increases in normal acceleration (n_z). The upper limit of linear maneuver stability military specification (80 lbf/n_z) is also shown in the figure.

The research proceeded as follows. First, the nonlinear F_c/n_z was made linear by two methods.

Second, pilot opinions for each of the two methods were recorded and compared with the military standard. Third, a break in the slope of the linear F_c/n_z characteristics was introduced and the opinion of the pilot of several initial and final slope pairs were recorded. Finally, a few cases with two slope breaks in the linear F_c/n_z characteristics were evaluated by the pilots.

An objective of this study was to evaluate a broad spectrum of linear and nonlinear longitudinal stability characteristics to generate data for defining satisfactory and unacceptable maneuver characteristics as defined by the opinions of the pilots. This study was a joint venture of NASA, the Federal Aviation Administration, and Lockheed Corporation with four pilots participating: one from NASA, one from the FAA, and two from Lockheed.

Symbols

Measurements and calculations were made in U.S. Customary Units, and all calculations are based on airplane body axes.

$\bar{c}$	mean aerodynamic chord, ft
c.g.	airplane center of gravity, ft
F_c	column force, lbf
$F_{c,\max}$	maximum column force, lbf
$F_{c,\min}$	minimum column force, lbf
g	acceleration due to gravity, $1g = 32.17$ ft/sec^2
K_{FF}	feedforward gain
K_q	pitch-rate damper gain
M	Mach number
n_z	normal acceleration, g units
q	pitch rate, deg/sec
SM	static margin, percent
s	Laplace transform operator
δ_c	column deflection, in.
$\delta_{c,\mathrm{MTC}}$	column deflection due to Mach trim compensation, in.
$\delta_{c,\mathrm{PACS}}$	column deflection (software only) due to pitch active control system, in.
$\delta_{c,p}$	column deflection due to pilot force input, in.
$\delta_{c,\mathrm{trim}}$	column deflection due to pilot trim beeper input, in.
δ_{col}	software stick position, in.
$\delta_{\mathrm{col,trim}}$	column deflection due to total trim and pilot force, in.
δ_H	horizontal-tail deflection, deg
τ	time constant, sec
τ_{lag}	pitch damper lag, sec
ϕ	bank angle, deg

Abbreviations:

AACS	aileron active control system
CHR	Cooper-Harper ratings
FAA	Federal Aviation Administration
FAR	Federal Aviation Regulations
IMC	instrument meteorology conditions
PACS	pitch active control system
PIO	pilot-induced oscillation
SAS	stability augmentation system
VMS	Visual/Motion Simulator

Description of Simulated Airplane

The Lockheed L-1011 airplane with extended wing span is a current generation, subsonic, commercial transport airplane (fig. 2). The airplane is powered by three Rolls-Royce 211-225 high-bypass-ratio turbofan engines and has a flying stabilizer with a geared elevator. During these simulations the aileron active control system (AACS) was inoperative. Airplane geometry and weight data are presented in table I.

The simulated L-1011 airplane uses a flying stabilizer for longitudinal control, inboard and outboard ailerons and spoilers for lateral control, and a rudder for directional control. The basic longitudinal control system includes a servoactuator, cable stretch, and position- and rate-limiter modeling. The lateral control system also includes a servoactuator and position-limiter modeling. Only spoiler panels 2 and 4 to 6 were modeled for lateral control (fig. 2(b)). Spoiler panel 1 is for ground use and spoiler panel 3 is operated only with AACS, which was not used for this study. The directional control system determines manual and stability augmentation system (SAS) contributions to rudder position. The directional SAS consists of a yaw damper and a

wheel-driven aileron and rudder interconnection for improved turn coordination.

For this study, servoactuator and rate- and position-limiter modeling were also used. The pitch active control system (PACS) provided acceptable flying qualities for negative static margins to 5 percent. The maneuver stability characteristics of the simulated aircraft were nonlinear (fig. 1). For this study, the column force per normal acceleration was made linear by one of two different methods: a nonlinear control loading with constant stick to tail gearing or a nonlinear tail gearing with constant stick force per inch control loading.

Description of Simulation Equipment

This study was made in the general-purpose cockpit of the Langley Visual/Motion Simulator (VMS), a ground-based six-degree-of-freedom motion simulator. For this study, the VMS had a transport-type cockpit equipped with conventional flight and engine-thrust controls and a flight-instrument display representative of the control panel found in current transport airplanes. (See fig. 3.) Instruments that indicate angle of attack, sideslip angle, flap angle, horizontal-stabilizer angle, and column force were also provided. A digital normal acceleration indicator was located on the instrument panel adjacent to the control column force meter, and a digital Mach meter was provided on an extended instrument panel above the conventional panel.

The control forces on the wheel, column, and rudder pedals were provided by a hydraulic system coupled with an analog computer. The system allowed for the usual characteristics of stiffness, damping, coulomb friction, breakout forces, detents, and inertia. No visual cues from outside were required for this study; therefore, evaluations were conducted under instrument meteorology conditions (IMC).

The average motion delay of the VMS, including computational time, is less than 70 msec. The washout system used to present motion-cue commands to the motion base is nonstandard and was conceived and developed at Langley (ref. 4). The washout system continuously adapts to parameter changes to (1) minimize a cost functional through continuous steepest descent method and (2) produce motion cues for translational accelerations and rotational rates within the motion envelope of the synergistic base.

Aural cues included engine noise and a tone that beeped intermittently at $1.5g$ and increased to a solid tone at $2.0g$. This tone signaled g units in wind-up turns.

Tests and Procedures

To generate data for acceptable maneuver characteristics, this study evaluated a broad spectrum of linear and nonlinear longitudinal control characteristics that are unique to nonlinear, swept-wing, high-subsonic, jet transport aircraft. The objective was to develop a database for acceptable maneuver stability characteristics for FAR Part 25 (regulations on engineering guidance). Various maneuver stability characteristics were defined by a mathematical model of an L-1011 aircraft for the piloted tests (ref. 5). Only a nominal, cruise flight condition was considered (Weight = 360 000 lbf, Altitude = 31 000 ft, $M = 0.83$). The basic maneuver stability (F_c/n_z) characteristics were systematically varied by (1) moving the aircraft center of gravity (c.g.) location, (2) changing the pitch-rate feedback multiplier gain (K_q) of the near-term PACS (fig. 4 and ref. 2), (3) changing the F_c/δ_c, and (4) changing the δ_H/δ_c. The basic longitudinal control system is described in reference 2. When F_c/δ_c was varied, δ_H/δ_c was set to a constant $-1.0°$/in. Conversely, when δ_H/δ_c was varied, F_c/δ_c was set to a constant 15.77 lbf/in. These conditions allowed F_c/n_z to be varied as shown in figure 5 instead of following the baseline nonlinear schedule shown in figure 1. A digital normal acceleration indicator was located on the instrument panel adjacent to a control column force meter to verify the linearity of F_c/n_z.

Seven aircraft c.g. locations were simulated, which represented static margins from approximately 33 percent (c.g. = $0.12\bar{c}$) to -5 percent (c.g. = $0.50\bar{c}$). Factors that were considered in the selection of maneuver stability characteristics are indicated in figure 5. The configurations evaluated are indicated in table II. Although 176 configurations are indicated in the table, configurations 22 through 27 and 46 through 51 were not evaluated. All configurations were not evaluated by all pilots. Table III summarizes the configurations evaluated by each pilot.

For each configuration, the pilot completed the comment card (fig. 6) by assigning a Cooper-Harper rating (CHR) to each maneuver (ref. 6 and fig. 7) and by commenting on the tendency toward pilot-induced oscillation (PIO). The pilot was asked to perform and evaluate the following four primary tasks:

1. Trimmability: Evaluate the ease or difficulty to initially trim the aircraft and to recapture trim from a disturbed condition.
2. Small pitch-attitude changes: Evaluate attitude stability when pitch attitude is changed and held with column force only.

3. Operational turns: Evaluate turn entry and exit characteristics when 30° to 40° banked turns are performed at constant airspeed with column force used to control attitude and altitude. Airspeed should be maintained within 5 knots, altitude should be maintained within 100 ft, and a 30° banked turn should produce $1.15g$.

4. Wind-up turns: Evaluate maneuver force and stability characteristics during wind-up turns. This emergency maneuver is performed at maximum power by rolling to a 60° banked turn with a minimum of $2g$ and without losing altitude or stalling the airplane.

Results and Discussion

Center of Gravity and Pitch-Rate Damping

The first 21 configurations were evaluated to determine the effects of c.g. and pitch-rate damping on the maneuver stability characteristics of the mathematical model of the basic airplane. As expected, increasing pitch-rate damping increased F_c/n_z, and moving the c.g. aft decreased F_c/n_z. (See fig. 8.) The evaluation of these 21 configurations for pilot 1 is also indicated in figure 8. The average ratings of all pilots who flew the configurations are given in table II. These results indicate that when pitch-rate damping was high, pilot 1 rated F_c/n_z as acceptable (CHR < 6.5), although the maneuver stability was nonlinear. Also, with $K_q = 2$, the F_c/n_z was rated within the satisfactory (CHR < 3.5) linear limits of references 7 and 8. However, to maintain level 1 short-period damping ratio, K_q should be less than 2 for c.g. locations forward of approximately $0.40\bar{c}$ (fig. 9). Also, maintaining K_q as high as possible is advantageous for phugoid stability (fig. 10). Therefore, for configurations 28 through 176 (table II), all tests were performed at the highest possible K_q for phugoid suppression while retaining level 1 short-period characteristics.

Linear Maneuver Stability

Before determining acceptable levels of nonlinear maneuver stability, the validity of current military level 1 boundaries for linear F_c/n_z must first be tested (refs. 7 and 8). (Boundaries for F_c/n_z are the same in refs. 7 and 8). For an L-1011 airplane with a limit load factor of 2.5, these boundaries are 23.3 lbf/g and 80.0 lbf/g. Figure 11 presents overall pilot ratings and associated trend curves for linear F_c/n_z obtained by varying F_c/δ_c with δ_H/δ_c constant. These overall ratings include all tasks performed by each pilot. (Pilot ratings of individual tasks are presented subsequently in the discussion.) Figure 12 indicates overall pilot ratings for linear F_c/n_z obtained by varying δ_H/δ_c, with F_c/δ_c constant. For both the variable F_c/δ_c and δ_H/δ_c conditions, K_q, was set at 2.0 (highest tested value) for improved phugoid damping. The short-period frequency and damping characteristics were within the level 1 boundaries of reference 7. The trend curves indicated in figures 11 and 12 were visually fitted through the available data points. Because data for the highly stable configurations (c.g. forward of $0.40\bar{c}$) were limited, the analysis concentrated on configurations with low static margins ranging from 5 percent (c.g. $= 0.40\bar{c}$) to -5 percent (c.g. $= 0.50\bar{c}$). The PIO tendencies were evident primarily at low maneuver stability levels. Typical of these was configuration 34 with c.g. $= 0.40\bar{c}$ and 15 lbf/g. This configuration evoked comments about PIO such as "Oscillations tend to develop when pilot initiates abrupt maneuvers or attempts tight control."

The overall pilot ratings shown in figures 11 and 12 are replotted in figure 13 for comparison of techniques used to maintain linear maneuver stability. The level 1 maneuver stability boundaries of reference 7 are also indicated in figure 13. The two methods used for varying F_c/n_z and maintaining a linear slope show little difference in the lower F_c/n_z range for c.g. locations of $0.40\bar{c}$ and $0.45\bar{c}$. (No conclusions were drawn for the statically unstable configuration, c.g. $= 0.50\bar{c}$, because all available data for the variable F_c/δ_c method were within level 1 boundaries of ref. 7.) However, the pilots seemed to be more sensitive to variations in F_c/δ_c than to variations in δ_H/δ_c in the upper F_c/n_z range. The implication is that a design with inadequate maneuver stability characteristics can be improved more readily through variations in F_c/δ_c than in δ_H/δ_c. However, these two parameters are definitely coupled. That is, an acceptable range of δ_H/δ_c at a specific value of F_c/δ_c may not be acceptable at a different value of F_c/δ_c.

The trend curves of figure 13 also indicate an optimum linear maneuver stability level of approximately 50 to 60 lbf/g for the subject configuration. In addition, a degradation of pilot ratings at extreme values of F_c/n_z is indicated and is most severe as column forces become lighter (i.e., reduction in F_c/n_z from optimum of 50 to 60 lbf/g).

For each configuration, the pilots rated individual tasks such as operational turns ($g < 1.5$) and wind-up turns ($g > 1.5$) (fig. 6). Pilot ratings for operational turns and wind-up turns are presented in figure 14 for variable F_c/δ_c and in figure 15 for δ_H/δ_c configurations. Trend curves were fitted

visually through the data. Again, it appears that degradation in pilot ratings is more severe in lower F_c/n_z regions particularly when the variable δ_H/δ_c method is used (fig. 15). The pilot comments also indicated a PIO tendency for low F_c/n_z configurations.

For the small pitch-attitude changes and operational turns using the variable (F_c/δ_c) method, the pilot ratings were consistently good for statically stable (c.g. = $0.40\bar{c}$) and neutrally stable (c.g. = $0.45\bar{c}$) configurations (fig. 14). These configurations were degraded by extreme F_c/n_z levels only for high-load-factor pilot tasks (i.e., for wind-up turns). However, statically unstable configurations (c.g. = $0.50\bar{c}$) appeared to be degraded at the extreme maneuver stability levels for all pilot tasks, including the small pitch-attitude changes and operational turns when the δ_H/δ_c method was used (fig. 15). The pilot ratings for small pitch-attitude changes were the same as the ratings for operational turns for the configurations in figures 14 and 15.

Based on a maximum level 1 Cooper-Harper rating of 3.5, the level 1 boundaries suggested by the results of the linear maneuver stability portion of this study are summarized in table IV. These results are based on both overall and individual pilot task ratings indicated in figures 13 to 15. Although the limited results of this study preclude determination of suggested maneuver stability boundaries, for this particular aircraft, a shift of approximately 10 lbf/g higher for values of F_c/n_z for minimum and maximum level 1 maneuver stability boundaries found in references 7 and 8 appears to be appropriate.

Nonlinear Maneuver Stability

Although pilots prefer linear F_c/n_z, providing such characteristics is sometimes difficult because of relaxed static stability in transports with advanced control systems. The degree of nonlinearity in maneuver stability characteristics acceptable to the pilots was evaluated during this study by parametric variations of F_c/n_z slope and are presented in figures 16 and 17. F_c/n_z variations with a single break at $n_z = 1.333g$ or $1.667/g$ with an initial slope of 50 lbf/g. This initial part of the slope falls in the midrange of acceptable values as specified in reference 7 for level 1 flying qualities. The slopes of F_c/n_z were controlled through either F_c/δ_c or δ_H/δ_c.

Figures 18 through 21 present pilot ratings for configurations with a single break in the F_c/n_z curves at either $n_z = 1.667g$ or $n_z = 1.333g$ with the static margins ranging from 5 percent to -5 percent. The trend curves fitted through these data are replotted and presented in figure 22 for comparing the effects of F_c/δ_c with δ_H/δ_c. These trend curves indicate that the pilots preferred a linear F_c/n_z variation for low-load-factor tasks (optimum pilot ratings at approximately 50 lbf/g, which implies no break), but they preferred a slight reduction in slope above $n_z = 1.667g$. For the configuration with c.g. = $0.50\bar{c}$ and SM = -5 percent with variable δ_H/δ_c, the pilots preferred a reduction in F_c/n_z slope from 50 lbf/g to 30 lbf/g at $n_z = 1.667g$. Also, with the break at $n_z = 1.333g$, the pilots strongly preferred an increase in slope over a reduction in slope, as indicated by a more rapid increase in pilot ratings with reduced slope after the break. The effect of slope reduction was much more noticeable to the pilots than the effect of slope increase, especially when the slope was near zero or negative (fig. 5). However, with the break at $n_z = 1.667g$, the pilot rating curves were fairly symmetrical about an optimum second slope value (fig. 28).

A comparison of the two methods used to modify the maneuver stability characteristics (fig. 22) shows little difference at low F_c/n_z values with the break at $n_z = 1.333g$ for all c.g. locations evaluated. When the break occurred at $n_z = 1.667g$ (fig. 22), the pilots had a slight preference for the F_c/δ_c method for statically stable (c.g. = $0.40\bar{c}$) and neutrally stable (c.g. = $0.45\bar{c}$) configurations. However, for the statically unstable configuration (c.g. = $0.50\bar{c}$), the pilots had a strong preference for the δ_H/δ_c method.

These results probably depend on the value selected for the fixed parameter (either δ_H/δ_c or F_c/δ_c) and only provide a single test point in what should be a more detailed analysis. However, this comparison provides insight into the proper means of linearizing the maneuver stability characteristics of a control system with inherent nonlinear maneuver stability. However, this study did not provide sufficient data to conclude which method is better.

In addition to the overall Cooper-Harper ratings for each configuration, separate ratings were obtained for each task. Figures 23 through 26 present pilot ratings for configurations with static margins of 5 percent and -5 percent and a single break in the F_c/n_z curve for the operational turn ($n_z \leq 1.4g$) and wind-up turn ($n_z \leq 2.0g$) tasks. These are the same configurations for which overall pilot ratings were presented in figures 18 through 21. Pilot ratings of the small pitch-attitude changes were consistently good and, therefore, are not presented. This task did not explore maneuver stability regions affected by the breaks evaluated in this study. The data of figures 23 through 26 are replotted in figure 27 for comparison.

Figure 27 indicates by favorable pilot ratings for the operational turns task with the break at $n_z = 1.667g$ that when the pilot evaluation task occurs in the linear portion of the maneuver stability curve, no degradation in flying qualities is detected. However, when the task called for maneuvering beyond the break point (in either direction), large changes in maneuver stability resulted in poor pilot ratings. Even large increases in maneuver stability from $n_z = 1.333g$ had little effect on pilot ratings for the operational turns with the statically unstable configuration (c.g. $= 0.50\bar{c}$). (The only augmentation for this simulated aircraft was an electronic pitch-rate damper.) With the task performed at a maximum load factor of $1.4g$, column forces had not yet become unreasonably high; thus, maneuver stability (F_c/n_z) increases were still undetected. The pilots were not seriously affected by large increases in maneuvering stability at $n_z = 1.333g$ for any tasks performed with the unstable (c.g. $= 0.50\bar{c}$) configuration. However, severe degradations in pilot ratings are indicated with the statically stable (c.g. $= 0.40\bar{c}$) configuration. Likewise, reductions in F_c/n_z slopes at $n_z = 1.333g$ brought about large degradations in pilot ratings for both the stable and the unstable configuration.

The question arises as to whether the pilot rating degradations due to abrupt changes in maneuver stability (F_c/n_z slope) were actually caused by the change in stability or by the fact that column forces may be approaching unacceptable values, as indicated in figures 16 and 17. Comments indicated that the pilots frequently did not detect a change in control characteristics at the actual break point, but rather as the column force approached established level 1 maneuver stability boundaries. For example, when the slope of F_c/n_z at $n_z = 1.667g$ changed from 50 lbf/g to -40 lbf/g, degradation in flying qualities was detected as the column force approached the lower level 1 boundary ($1.9g$), instead of where the actual break occurred. (See fig. 16.) Pilot comments frequently suggested that the break occurred near level 1 boundaries, not where the actual break occurred. Configurations that actually did have a break in the F_c/n_z curve, but did not cross level 1 boundaries were typically rated as satisfactory. When the slope was -10 lbf/g after the break at $n_z = 1.667g$ is one example (fig. 16). A second example, with a slope of 80 lbf/g after the break produced comments such as "a little heavy but very flyable."

Pilot ratings for double-break maneuver stability variations (fig. 28 and configurations 152 through 170 of table II) were acquired but were insufficient for detailed analysis. Initial pilot ratings indicated no improvements over single-break configurations and for the sake of brevity were limited to at least one pilot flying each configuration.

Near the conclusion of this study, the primary project pilot was asked to design what he believed would be the optimum maneuver stability curve for this particular airplane. The result is presented in figure 29, but because of insufficient evaluations no analysis was made of the F_c/n_z characteristic. This pilot opted for three distinct values for F_c/n_z instead of a constant value. He chose a nominal value of 45 lbf/g, then a reduction of 40 percent to 27 lbf/g between $n_z = 1.15g$ ($\phi \approx 30°$) and $1.6g$ ($\phi \approx 50°$), and finally an increase in F_c/n_z to 65 lbf/g beyond $n_z = 1.6g$.

Concluding Remarks

NASA, Federal Aviation Administration, and Lockheed Corporation performed a cooperative flight simulation experiment in the six-degree-of-freedom, ground-based Langley Visual/Motion Simulator (VMS). An objective of the study was to provide engineering guidance for acceptable nonlinear maneuver stability characteristics for transport aircraft. The baseline mathematical model of the airplane represented a wide-body jet transport with a pitch-active control system (PACS). The PACS provided acceptable flying qualities for negative static margins to 5 percent. The maneuver stability characteristics were modified through systematic variations of PACS pitch-rate damper gain, aircraft center of gravity, control loading (column force per column deflection (F_c/δ_c)), and control gearing (horizontal-tail deflection per control force (δ_H/δ_c)). The evaluation tasks consisted of performing (1) pitch-attitude changes, (2) standard operational turns, and (3) wind-up turns, at a representative flight condition in calm atmospheric conditions.

The current military specifications dictate minimum and maximum levels of maneuver stability (column force per normal acceleration, F_c/n_z) for level 1 (satisfactory) flying qualities. These boundaries are 23.3 lbf/g and 80.0 lbf/g, respectively, for the baseline airframe used in this study. The results of this experiment verify the specification boundaries, with only a slight possible shift toward higher (by approximately 10 lbf/g) column forces recommended for this type of aircraft. However, the present specification level 1 boundaries appear to be reasonable.

A degradation in pilot ratings at extreme values of F_c/n_z was evident for all pilot tasks for statically unstable configurations evaluated. However, the statically stable configurations appear to be degraded

only in high-load-factor pilot tasks (e.g., wind-up turns).

The maneuver stability was made linear by either adjusting F_c/δ_c or δ_H/δ_c. The results indicated that variations in δ_H/δ_c rather than F_c/δ_c, to maintain linear F_c/n_z provided improved longitudinal flying qualities in the upper F_c/n_z range but provided no advantage in the lower range. However, these two parameters are coupled; that is, an acceptable range of δ_H/δ_c at a fixed value of F_c/δ_c may not be acceptable at another value of F_c/δ_c.

While this research was comprehensive, some configurations were tested by only one or two pilots and these configurations may deserve further investigation.

NASA Langley Research Center
Hampton, VA 23681-0001
December 15, 1993

References

1. Airworthiness Standards: Transport Category Airplanes. FAR, Pt. 25, Federal Aviation Adm., June 1974.

2. Grantham, William D.; Person, Lee H., Jr.; Brown, Philip W.; Becker, Lawrence E.; Hunt, George E.; Rising, J. J.; Davis, W. J.; Willey, C. S.; Weaver, W. A.; and Cokeley, R.: *Handling Qualities of a Wide-Body Transport Airplane Utilizing Pitch Active Control Systems (PACS) for Relaxed Static Stability Application.* NASA TP-2482, 1985.

3. Jagger, Douglas H.: New Technology in the A320. AIAA-84-2444, Oct. Nov. 1984.

4. Martin, D. J., Jr.: *A Digital Program for Motion Washout on Langley's Six-Degree-of-Freedom Motion Simulator.* NASA CR-145219, 1977.

5. Grantham, William D.; Smith, Paul M.; Person, Lee H., Jr.; Meyer, Robert T.; and Tingas, Stephen A.: *Piloted Simulator Study of Allowable Time Delays in Large-Airplane Response.* NASA TP-2652, 1987.

6. Cooper, George E.; and Harper, Robert P., Jr.: *The Use of Pilot Rating in the Evaluation of Aircraft Handling Qualities.* NASA TN D-5153, 1969.

7. Military Specification Flying Qualities of Piloted Airplanes. MIL-F-8785C, Nov. 5, 1980. (Supersedes MIL-F-8785B, Aug. 7, 1969.)

8. Military Standard Flying Qualities of Piloted Aircraft. MIL-STD-1797A, Jan. 30, 1990. (Supersedes MIL-STD-1797(USAF), Mar. 31, 1987.)

Table I. Airplane Geometry and Weight Data

Wing:	
Reference area, ft^2	3456
Reference mean aerodynamic chord, ft^2	24.46
Span, ft	164.33
Aspect ratio	7.817
Leading-edge sweep, deg	35
Horizontal tail:	
Area, ft^2	1282
Span, ft	71.58
Aspect ratio	4.0
Leading-edge sweep, deg	35
Vertical tail:	
Area, ft^2	550
Span, ft	29.67
Aspect ratio	1.6
Leading-edge sweep, deg	35
Weight:	
Maximum ramp, lbf	424 000
Maximum takeoff, lbf	422 000
Maximum landing, lbf	358 000
Cruise at 33 000 ft ($M = 0.83$), lbf	360 000
Zero fuel, lbf	312 460
Operating empty, lbf	261 000

Table II. Average Evaluations of Configurations

Configuration number	c.g.	SM	K_q	F_c/δ_c	δ_H/δ_c	F_c/n_z	No. of breaks	First break, n_z	Second slope, F_c/n_z	Second break, n_z	Third slope, F_c/n_z	Average CHR
1	0.12	33	0	Fixed	Fixed	Basic	0					3.5
2	0.12	33	1	Fixed	Fixed	Basic	0					3.0
3	0.12	33	2	Fixed	Fixed	Basic	0					3.5
4	0.25	20	0	Fixed	Fixed	Basic	0					5.0
5	0.25	20	1	Fixed	Fixed	Basic	0					3.5
6	0.25	20	2	Fixed	Fixed	Basic	0					3.5
7	0.35	10	0	Fixed	Fixed	Basic	0					6.0
8	0.35	10	1	Fixed	Fixed	Basic	0					5.5
9	0.35	10	2	Fixed	Fixed	Basic	0					3.5
10	0.40	5	0	Fixed	Fixed	Basic	0					9.0
11	0.40	5	1	Fixed	Fixed	Basic	0					6.0
12	0.40	5	2	Fixed	Fixed	Basic	0					3.5
13	0.45	0	0	Fixed	Fixed	Basic	0					10.0
14	0.45	0	1	Fixed	Fixed	Basic	0					6.5
15	0.45	0	2	Fixed	Fixed	Basic	0					3.5
16	0.47	−2	0	Fixed	Fixed	Basic	0					10.0
17	0.47	−2	1	Fixed	Fixed	Basic	0					7.0
18	0.47	−2	2	Fixed	Fixed	Basic	0					4.0
19	0.50	−5	0	Fixed	Fixed	Basic	0					10.0
20	0.50	−5	1	Fixed	Fixed	Basic	0					10.0
21	0.50	−5	2	Fixed	Fixed	Basic	0					5.5
22	0.12	33	0	Fixed	Variable	15	0					
23	↓	↓	↓	↓	↓	30	↓					
24						45						
25						60						
26						90						
27						120						
28	0.25	20	1	Fixed	Variable	15	0					6.0
29	↓	↓	↓	↓	↓	30	↓					3.5
30						45						3.0
31						60						3.0
32						90						4.0
33						120						6.0

Table II. Continued

Configuration number	c.g.	SM	K_q	F_c/δ_c	δ_H/δ_c	F_c/n_z	No. of breaks	First break, n_z	Second slope, F_c/n_z	Second break, n_z	Third slope, F_c/n_z	Average CHR
34	0.40	5	2	Fixed	Variable	15	0					6.0
35	↓	↓	↓	↓	↓	30	↓					4.5
36						45						3.0
37						60						3.0
38						90						3.5
39						120						4.0
40	0.45	0	2	Fixed	Variable	15	0					5.0
41	↓	↓	↓	↓	↓	30	↓					3.0
42						45						2.5
43						60						2.0
44						90						3.0
45						120						4.0
46	0.47	−2	2	Fixed	Variable	15	0					5.0
47	↓	↓	↓	↓	↓	30	↓					
48						45						
49						60						
50						90						
51						120						
52	0.50	−5	2	Fixed	Variable	15	0					6.5
53	↓	↓	↓	↓	↓	30	↓					5.0
54						45						3.5
55						60						3.0
56						90						4.0
57						120						5.0
58	0.12	33	0	Variable	Fixed	30	0					9.0
59	↓	↓	↓	↓	↓	45	↓					7.0
60						60						7.0
61						90						7.0
62	0.25	20	1	Variable	Fixed	30	0					3.0
63	↓	↓	↓	↓	↓	45	↓					3.5
64						60						3.5
65						90						4.0
66						120						7.0
67	0.40	5	2	Variable	Fixed	45	0					3.0
68	↓	↓	↓	↓	↓	60	↓					3.0
69						90						4.5
70						120						5.0

Table II. Continued

Configuration number	c.g.	SM	K_q	F_c/δ_c	δ_H/δ_c	F_c/n_z	No. of breaks	First break, n_z	Second slope, F_c/n_z	Second break, n_z	Third slope, F_c/n_z	Average CHR
71	0.45	0	2	Variable	Fixed	30	0					3.5
72	↓	↓	↓	↓	↓	45	↓					2.5
73	↓	↓	↓	↓	↓	60	↓					3.0
74	↓	↓	↓	↓	↓	90	↓					4.0
75	0.47	−2	2	Variable	Fixed	30	0					3.5
76	↓	↓	↓	↓	↓	45	↓					3.0
77	↓	↓	↓	↓	↓	60	↓					3.0
78	↓	↓	↓	↓	↓	90	↓					3.0
79	0.50	−5	2	Variable	Fixed	30	0					3.0
80	0.50	−5	2	Variable	Fixed	45	0					3.0
81	0.50	−5	2	Variable	Fixed	60	0					4.5
82	0.40	5	2	Fixed	Variable	Variable†	1	1.667	−70			10.0
83	↓	↓	↓	↓	↓	↓	↓	↓	−40			9.0
84	↓	↓	↓	↓	↓	↓	↓	↓	−10			6.5
85	↓	↓	↓	↓	↓	↓	↓	↓	20			3.0
86	↓	↓	↓	↓	↓	↓	↓	↓	80			3.0
87	↓	↓	↓	↓	↓	↓	↓	↓	170			8.0
88	0.45	0	2	Fixed	Variable	Variable	1	1.667	−70			10.0
89	↓	↓	↓	↓	↓	↓	↓	↓	−40			8.5
90	↓	↓	↓	↓	↓	↓	↓	↓	−10			7.0
91	↓	↓	↓	↓	↓	↓	↓	↓	20			3.0
92	↓	↓	↓	↓	↓	↓	↓	↓	80			3.5
93	↓	↓	↓	↓	↓	↓	↓	↓	170			8.0
94	0.50	−5	2	Fixed	Variable	Variable	1	1.667	−70			10.0
95	↓	↓	↓	↓	↓	↓	↓	↓	−40			8.5
96	↓	↓	↓	↓	↓	↓	↓	↓	−10			4.0
97	↓	↓	↓	↓	↓	↓	↓	↓	20			3.0
98	↓	↓	↓	↓	↓	↓	↓	↓	80			3.0
99	↓	↓	↓	↓	↓	↓	↓	↓	170			6.5
100	0.40	5	2	Variable	Fixed	Variable	1	1.667	−40			8.0
101	↓	↓	↓	↓	↓	↓	↓	↓	−10			4.0
102	↓	↓	↓	↓	↓	↓	↓	↓	−20			3.0
103	↓	↓	↓	↓	↓	↓	↓	↓	80			3.0
104	↓	↓	↓	↓	↓	↓	↓	↓	170			5.0

†Initial slope 50 lbf/g.

Table II. Continued

Configuration number	c.g.	SM	K_q	F_c/δ_c	δ_H/δ_c	F_c/n_z	No. of breaks	First break, n_z	Second slope, F_c/n_z	Second break, n_z	Third slope, F_c/n_z	Average CHR
105	0.45	0	2	Variable	Fixed	Variable	1	1.667	−40			8.0
106	↓	↓	↓	↓	↓	↓	↓	↓	−10			5.0
107	↓	↓	↓	↓	↓	↓	↓	↓	−20			2.5
108	↓	↓	↓	↓	↓	↓	↓	↓	80			4.0
109	↓	↓	↓	↓	↓	↓	↓	↓	170			5.0
110	0.50	−5	2	Variable	Fixed	Variable	1	1.667	−70			9.5
111	↓	↓	↓	↓	↓	↓	↓	↓	−40			7.0
112	↓	↓	↓	↓	↓	↓	↓	↓	−10			4.5
113	↓	↓	↓	↓	↓	↓	↓	↓	20			3.0
114	↓	↓	↓	↓	↓	↓	↓	↓	80			8.0
115	0.40	5	2	Fixed	Variable	Variable	1	1.333	−10			10.0
116	↓	↓	↓	↓	↓	↓	↓	↓	5			7.0
117	↓	↓	↓	↓	↓	↓	↓	↓	20			5.0
118	↓	↓	↓	↓	↓	↓	↓	↓	35			3.5
119	↓	↓	↓	↓	↓	↓	↓	↓	65			3.5
120	↓	↓	↓	↓	↓	↓	↓	↓	110			4.5
121	↓	↓	↓	↓	↓	↓	↓	↓	155			7.0
122	0.45	0	2	Fixed	Variable	Variable	1	1.333	−10			10.0
123	↓	↓	↓	↓	↓	↓	↓	↓	5			7.0
124	↓	↓	↓	↓	↓	↓	↓	↓	20			5.0
125	↓	↓	↓	↓	↓	↓	↓	↓	35			3.5
126	↓	↓	↓	↓	↓	↓	↓	↓	65			3.5
127	↓	↓	↓	↓	↓	↓	↓	↓	110			6.0
128	↓	↓	↓	↓	↓	↓	↓	↓	155			6.0
129	0.50	−5	2	Fixed	Variable	Variable	1	1.333	−10			10.0
130	↓	↓	↓	↓	↓	↓	↓	↓	5			7.0
131	↓	↓	↓	↓	↓	↓	↓	↓	20			6.0
132	↓	↓	↓	↓	↓	↓	↓	↓	35			3.0
133	↓	↓	↓	↓	↓	↓	↓	↓	65			3.0
134	↓	↓	↓	↓	↓	↓	↓	↓	110			4.0
135	↓	↓	↓	↓	↓	↓	↓	↓	155			5.0
136	0.40	5	2	Variable	Fixed	Variable	1	1.333	1			7.0
137	↓	↓	↓	↓	↓	↓	↓	↓	20			4.0
138	↓	↓	↓	↓	↓	↓	↓	↓	35			3.0
139	↓	↓	↓	↓	↓	↓	↓	↓	65			4.5
140	↓	↓	↓	↓	↓	↓	↓	↓	110			5.0
141	↓	↓	↓	↓	↓	↓	↓	↓	155			6.0

Table II. Concluded

Configuration number	c.g.	SM	K_q	F_c/δ_c	δ_H/δ_c	F_c/n_z	No. of breaks	First break, n_z	Second slope, F_c/n_z	Second break, n_z	Third slope, F_c/n_z	Average CHR
142	0.45	0	2	Variable	Fixed	Variable	1	1.333	5			6.0
143	↓	↓	↓	↓	↓	↓	↓	↓	20			5.0
144									35			3.5
145									65			3.5
146									110			3.5
147	0.50	−5	2	Variable	Fixed	Variable	1	1.333	−10			8.5
148	↓	↓	↓	↓	↓	↓	↓	↓	5			7.0
149									20			6.5
150									35			5.0
151									65			5.5
152	0.25	20	1	Fixed	Variable	Variable	2	1.333	0	1.667	−20	8.5
153	0.25	20	1	Fixed	Variable	Variable	2	1.333	20	1.667	20	7.0
154	0.25	20	1	Fixed	Variable	Variable	2	1.333	50	1.667	50	7.0
155	0.25	20	1	Fixed	Variable	Variable	2	1.333	−20	1.667	0	10.0
156	↓	↓	↓	↓	↓	↓	↓	↓	↓	↓	20	10.0
157											40	9.0
158											70	9.0
159	0.50	−5	2	Fixed	Variable	Variable	2	1.333	0	1.667	−20	10.0
160	0.50	−5	2	Fixed	Variable	Variable	2	1.333	0	1.667	20	6.0
161	0.50	−5	2	Fixed	Variable	Variable	2	1.333	0	1.667	50	6.0
162	0.50	−5	2	Fixed	Variable	Variable	2	1.333	−20	1.667	0	10.0
163	↓	↓	↓	↓	↓	↓	↓	↓	↓	↓	20	10.0
164											40	7.5
165											70	9.0
166	0.25	20	1	Variable	Fixed	Variable	2	1.333	0	1.667	20	8.0
167	0.25	20	1	Variable	Fixed	Variable	2	1.333	50	1.667	50	7.0
168	0.50	−5	2	Fixed	Variable	Variable	2	1.333	0	1.667	−20	5.0
169	0.50	−5	2	Fixed	Variable	Variable	2	1.333	20	1.667	−20	6.0
170	0.50	−5	2	Fixed	Variable	Variable	2	1.333	50	1.667	−20	6.0
171	0.40	5	2	Fixed	Variable	Variable	2	1.155	27	1.600	65	3.0
172	0.45	0	2	Fixed	Variable	Variable	2	1.155	27	1.600	65	3.0
173	0.50	−5	2	Fixed	Variable	Variable	2	1.155	27	1.600	65	3.5
174	0.40	5	2	Variable	Fixed	Variable	2	1.155	27	1.600	65	5.5
175	0.45	0	2	Variable	Fixed	Variable	2	1.155	27	1.600	65	3.5
176	0.50	−5	2	Variable	Fixed	Variable	2	1.155	27	1.600	65	5.0

Table III. Configurations Evaluated by Each Pilot

Configuration	Pilot 1	Pilot 2	Pilot 3	Pilot 4	Configuration	Pilot 1	Pilot 2	Pilot 3	Pilot 4
1	X			X	55	X	X	X	X
2	X			X	56	X	X	X	X
3	X			X	57	X	X	X	X
4	X	X	X	X	58	X			
5	X	X	X	X	59	X			
6	X	X	X	X	60	X			
7	X			X	61			X	
8	X			X	62	X			
9	X			X	63	X			
10	X	X	X	X	64	X			
11	X	X	X	X	65			X	
12	X	X	X	X	66			X	
13	X	X	X	X	67	X	X	X	X
14	X	X	X	X	68	X	X	X	X
15	X	X	X	X	69	X	X	X	X
16	X	X	X	X	70	X	X	X	X
17	X	X	X	X	71	X	X	X	X
18	X	X	X	X	72	X	X	X	X
19	X	X		X	73	X	X	X	X
20	X	X		X	74	X	X	X	X
21	X	X	X	X	75	X	X		
28	X		X		76	X	X		
29	X		X		77		X	X	
30	X		X		78		X	X	
31	X		X		79	X	X	X	X
32	X		X		80		X	X	X
33	X		X		81		X	X	X
34	X	X	X	X	82	X	X	X	
35	X	X	X	X	83	X	X	X	X
36	X	X	X	X	84	X	X	X	X
37	X	X	X	X	85	X	X	X	X
38	X	X	X	X	86	X	X	X	X
39	X	X	X	X	87	X	X	X	X
40	X	X	X	X	88	X	X		
41	X	X	X	X	89	X	X		
42	X	X	X	X	90	X	X		
43	X	X	X	X	91	X	X		
44	X	X	X	X	92	X	X		
45	X	X	X	X	93	X	X		
52	X	X	X	X	94	X	X	X	X
53	X	X	X	X	95	X	X	X	X
54	X	X	X	X	96	X	X		X

Table III. Concluded

Configuration	Pilot 1	Pilot 2	Pilot 3	Pilot 4	Configuration	Pilot 1	Pilot 2	Pilot 3	Pilot 4
97	X	X		X	139	X	X		X
98	X	X		X	140			X	
99	X	X	X	X	141			X	
100	X	X	X	X	142	X	X	X	
101	X	X	X	X	143	X	X	X	
102	X	X	X	X	144	X	X	X	
103	X	X	X	X	145			X	
104			X	X	146			X	
105	X		X	X	147	X	X	X	
106	X		X	X	148	X	X	X	X
107	X		X	X	149	X	X	X	X
108			X	X	150	X	X	X	X
109			X	X	151			X	
110	X		X		152	X			X
111	X	X	X	X	153	X	X		X
112	X	X	X	X	154	X	X		X
113	X	X	X	X	155	X			
114		X	X	X	156	X			
115	X	X			157	X	X		
116	X	X		X	158	X	X		
117	X	X			159	X		X	X
118	X	X		X	160	X	X	X	X
119	X	X			161	X	X		X
120	X	X		X	162	X			
121	X	X			163	X			
122	X	X			164	X	X		
123	X	X		X	165	X	X		
124	X	X			166	X	X		X
125	X	X		X	167	X	X		X
126	X	X			168	X			
127	X	X		X	169	X	X		X
128	X	X			170	X	X		X
129	X	X	X		171			X	
130	X	X	X	X	172	X		X	
131	X		X		173			X	
132	X	X	X	X	174			X	X
133	X	X	X		175	X		X	
134	X	X	X	X	176			X	X
135	X	X	X						
136	X	X		X					
137	X	X		X					
138	X	X		X					

Table IV. Linear Maneuver Stability Level 1 Boundaries of This Study and Military Specifications

Source	Static margin, percent	Technique used to linearize F_c/n_z	Force per acceleration, F_c/n_z, lbf/g-unit	
			Minimum	Maximum
Present study	5	Variable δ_H/δ_c	41	107
	0	Variable δ_H/δ_c	29	103
	−5	Variable δ_H/δ_c	31	82
	5	Variable F_c/δ_c	39	85
	0	Variable F_c/δ_c	27	74
	−5	Variable F_c/δ_c		
Military Specifications (refs. 7 and 8)			[a]33.4	[a]90.2
			23.3	80.0

[a]Average

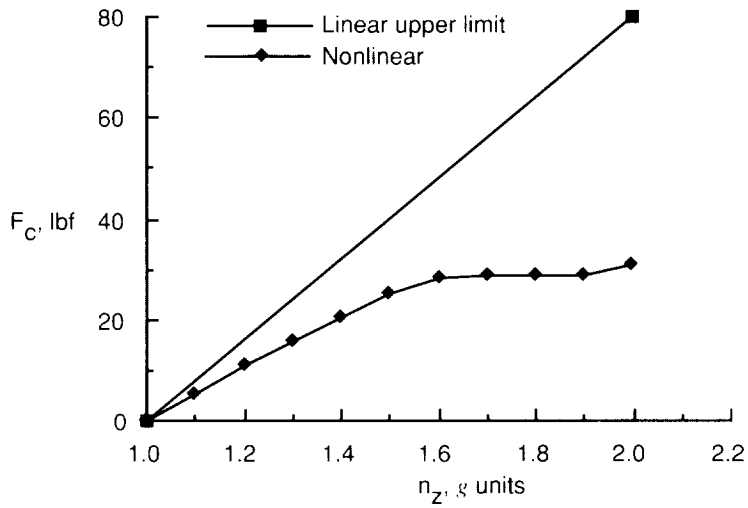

Figure 1. Maneuver stability characteristics.

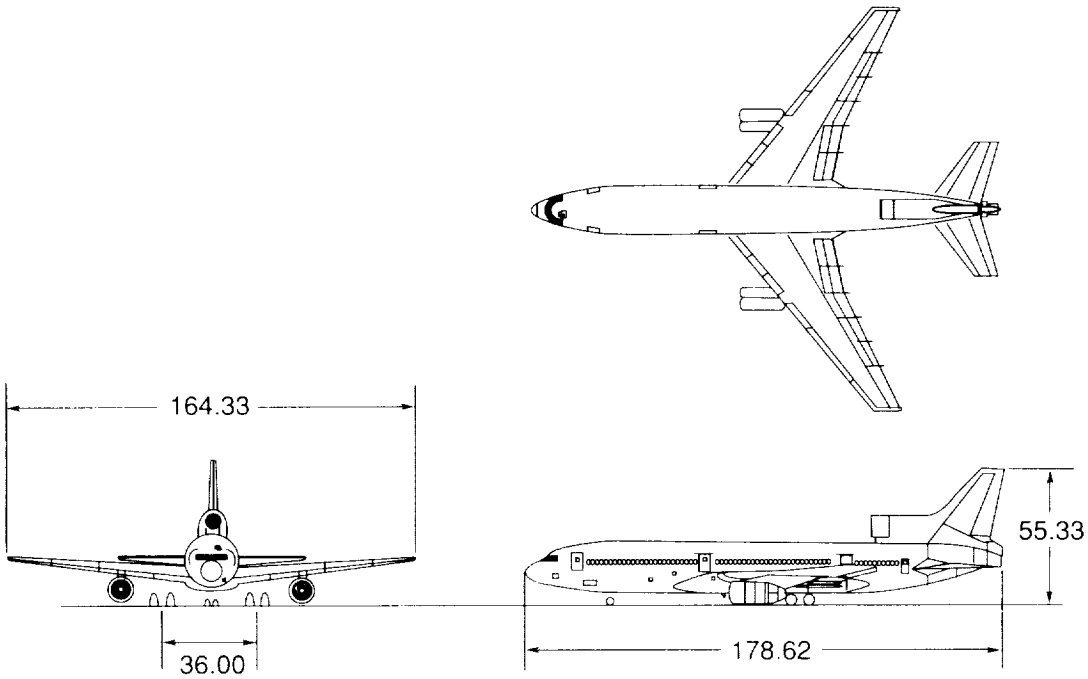

(a) Three-view sketch.

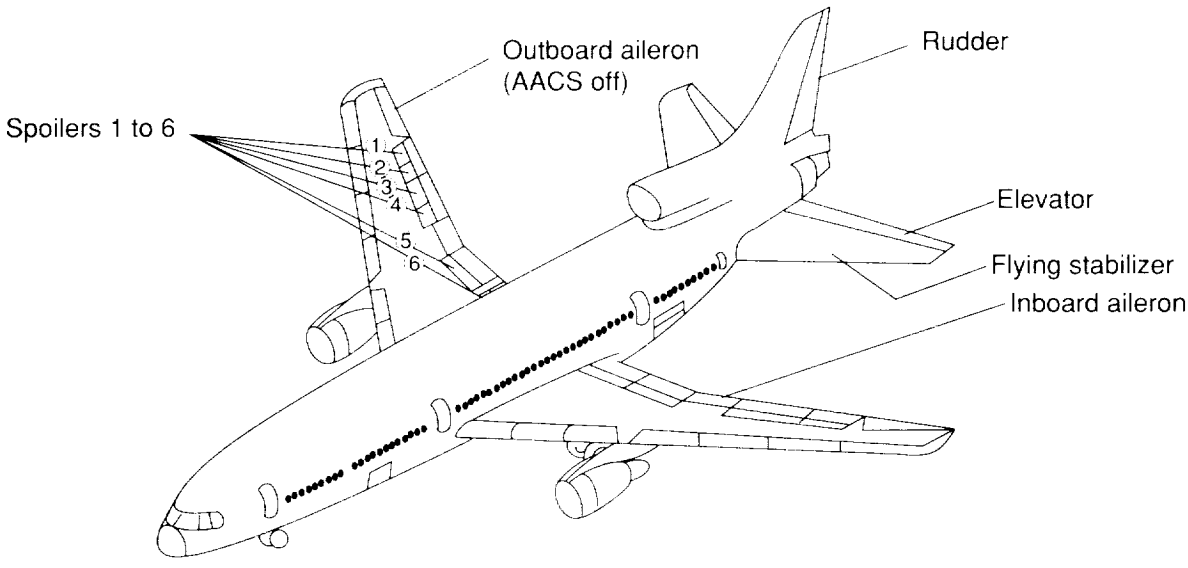

(b) Control surfaces.

Figure 2. Lockheed L-1011 airplane. All dimensions indicated are in feet.

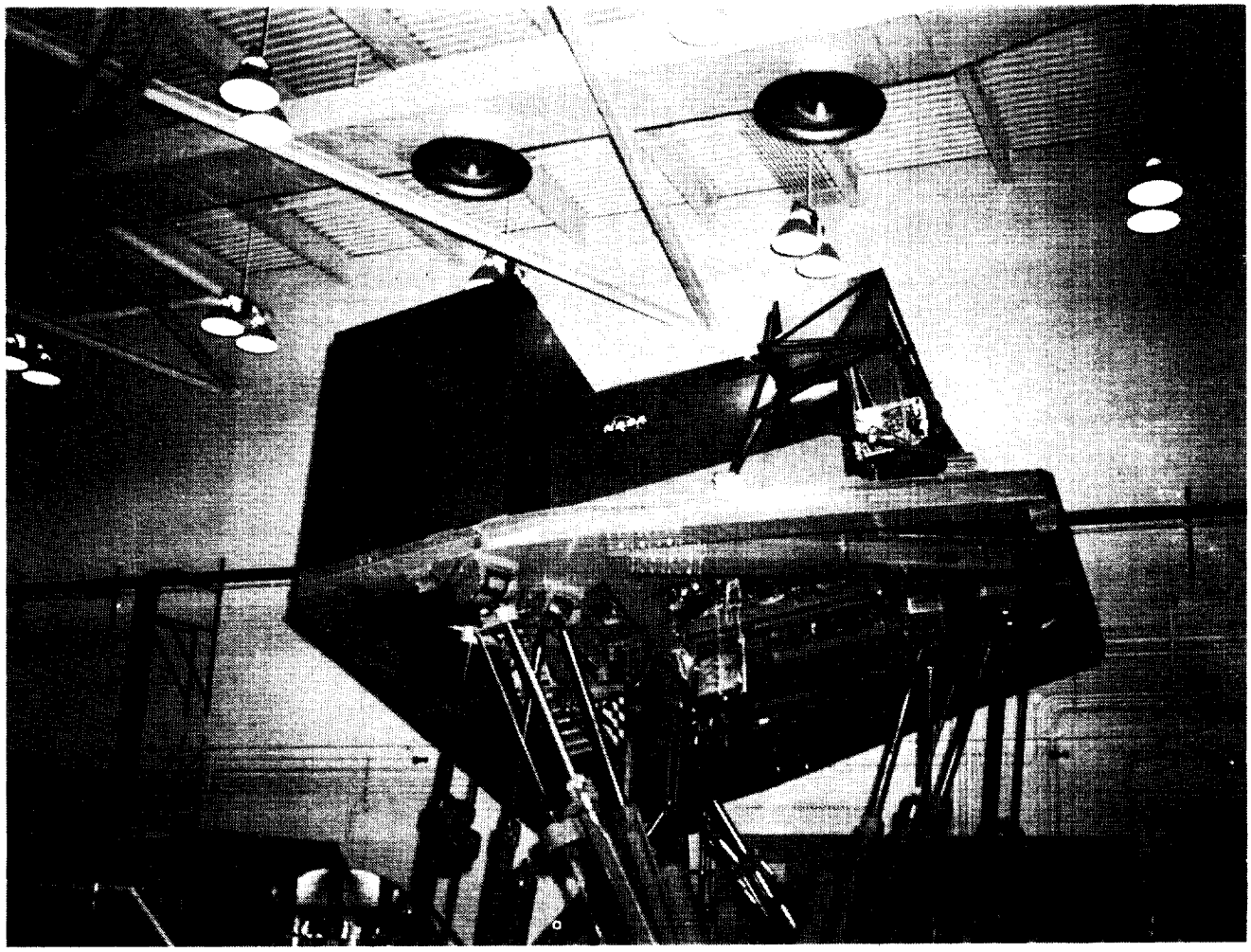

L-75-7570

(a) Langley Visual/Motion Simulator.

Figure 3. Langley Visual/Motion Simulator and instrument panel display.

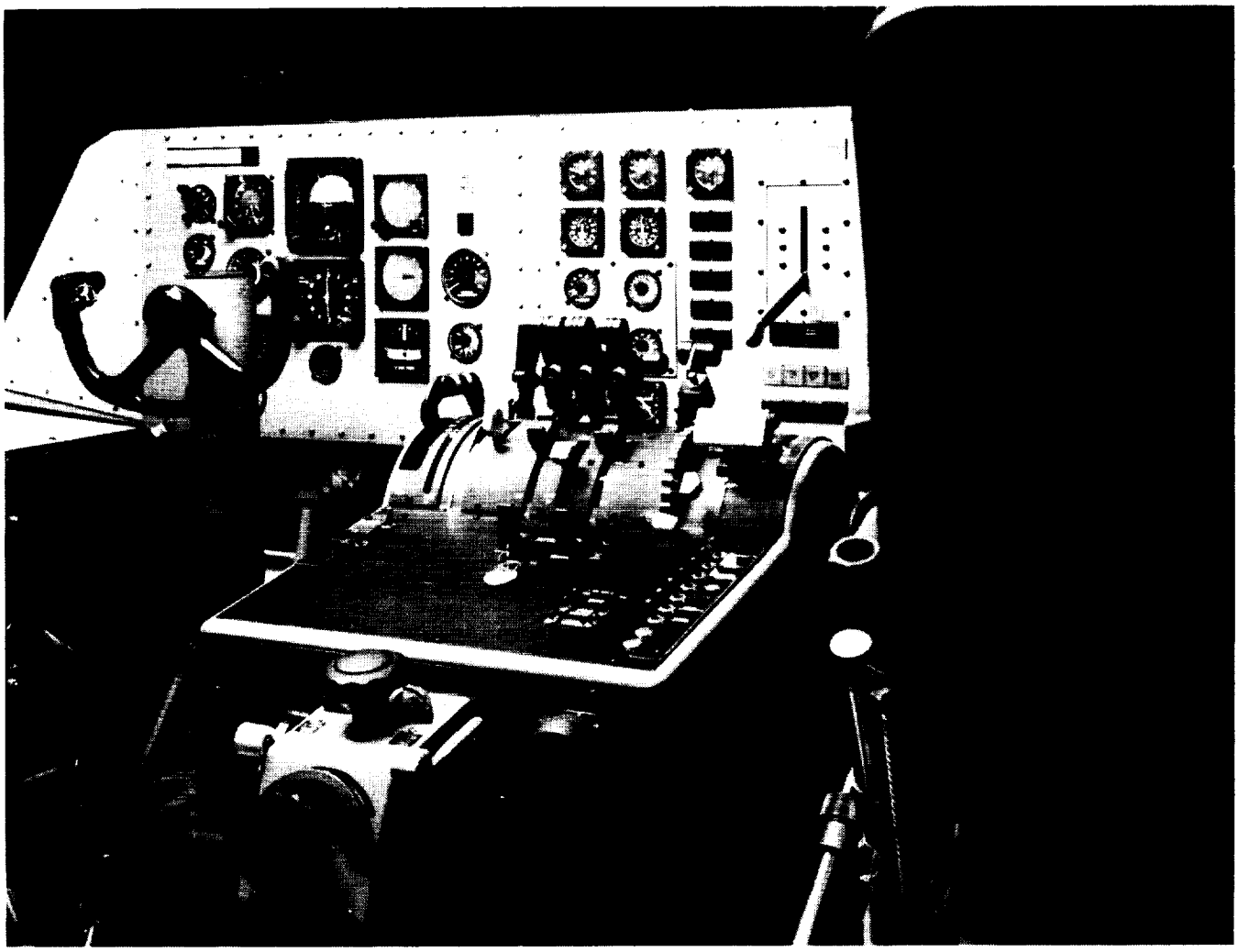

L-78-7794

(b) Instrument panel.

Figure 3. Concluded.

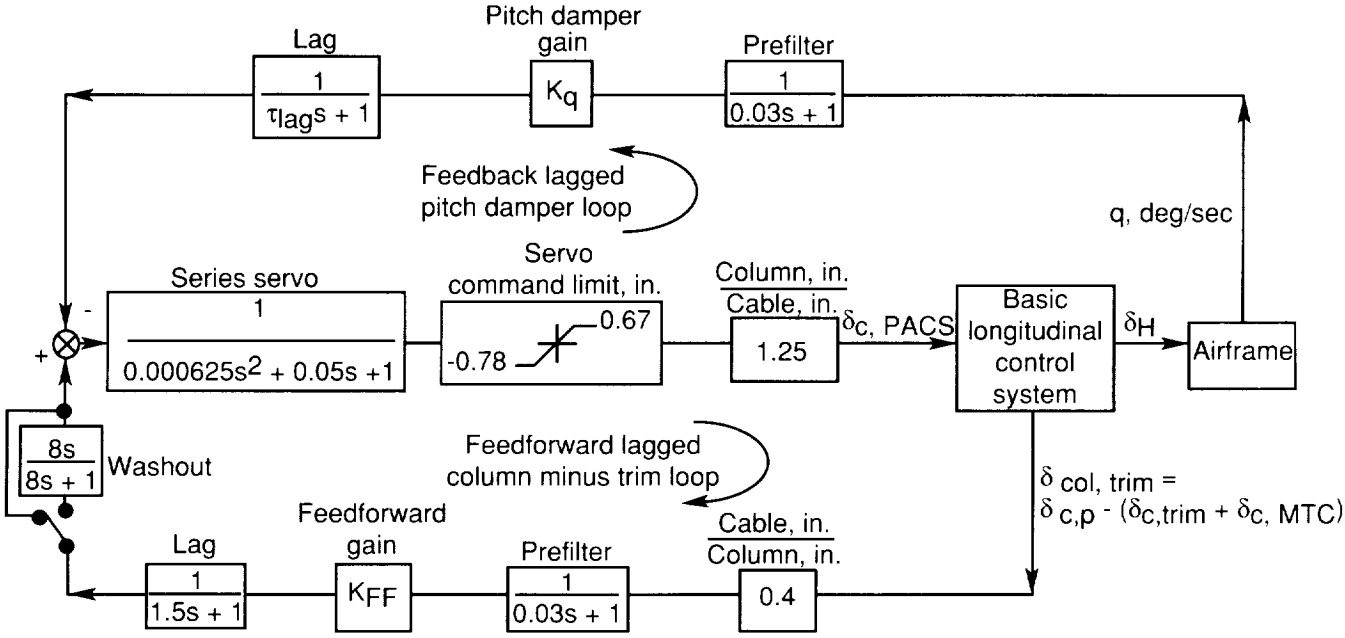

Figure 4. Analytical diagram of near-term PACS.

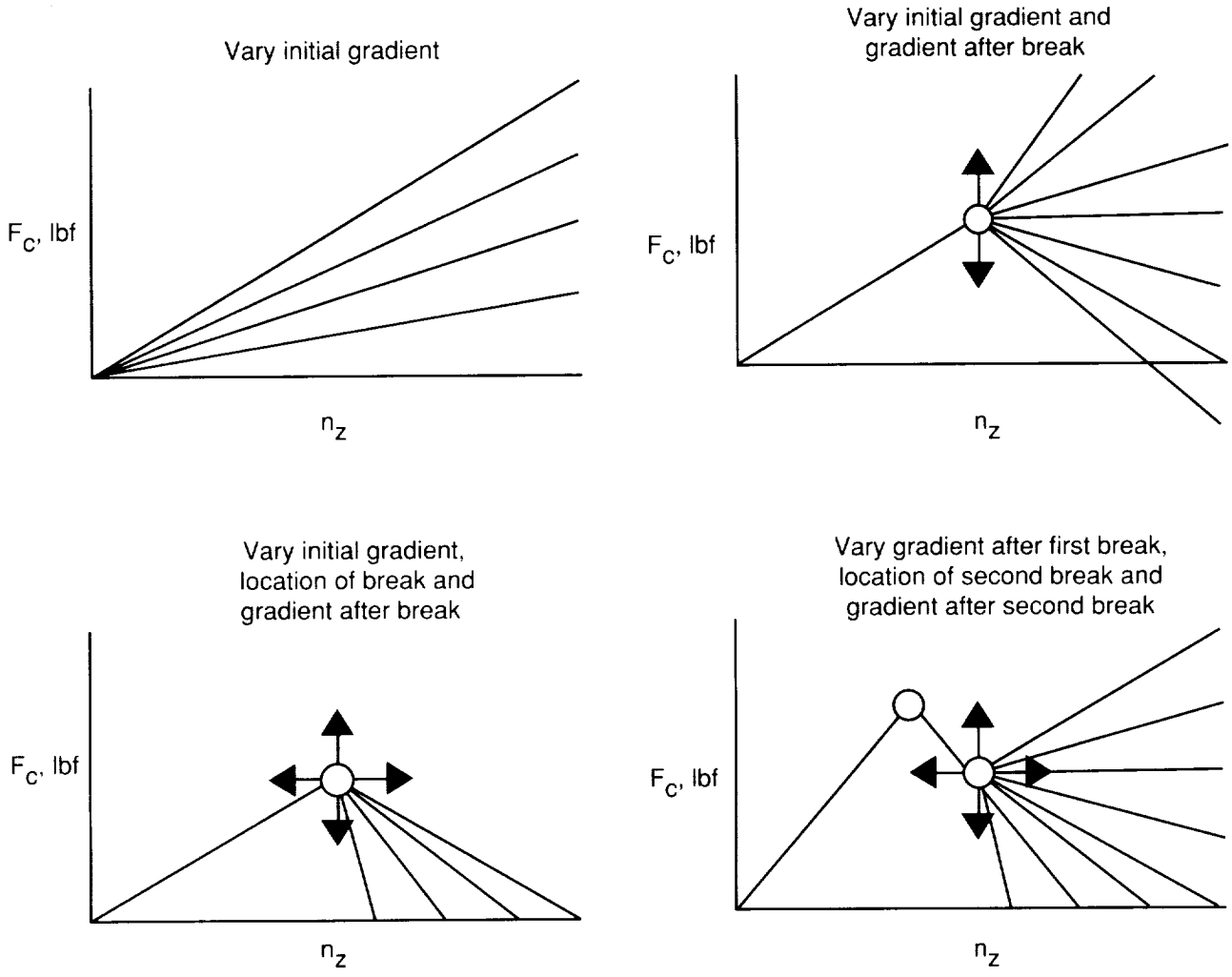

Figure 5. Possible maneuver stability characteristics for piloted flight simulation evaluation.

DATE:_____CONFIGURATION:_____PILOT:_____

1. TRIMMABILITY:-

2. SMALL PITCH CHANGES:
   Initial response:-

   Damping:-

   Predictability /Precision:-

   PIO:-

   Cooper-Harper_____Major Reason:-

3. OPERATIONAL TURNS (g < 1.5):

   Entry/exit characteristics:-

   Ability to hold altitude (±100'):-

   Tendency to PIO:-

   Stick Force Characteristics:-

   Special techniques:-

   Cooper-Harper_____Major reason:-

4. WIND-UP TURNS (g >1.5):

   Ability to attain/stabilize desired load factor:-

   Tendency to PIO:-

   Maneuver Force Characteristics;

      Predictability:-

      Forces:-

      Disp:-

      Sens:-

      Linearity:-

   Special Techniques:-

   Cooper-Harper_____Major reason:-

SUMMARY:

   Good Features:-

   Major Problems:-

   Overall Cooper-Harper_____.

   Overall PIO: Rating_____Task_____.

   Phugoid:-

Figure 6. Pilot comment card.

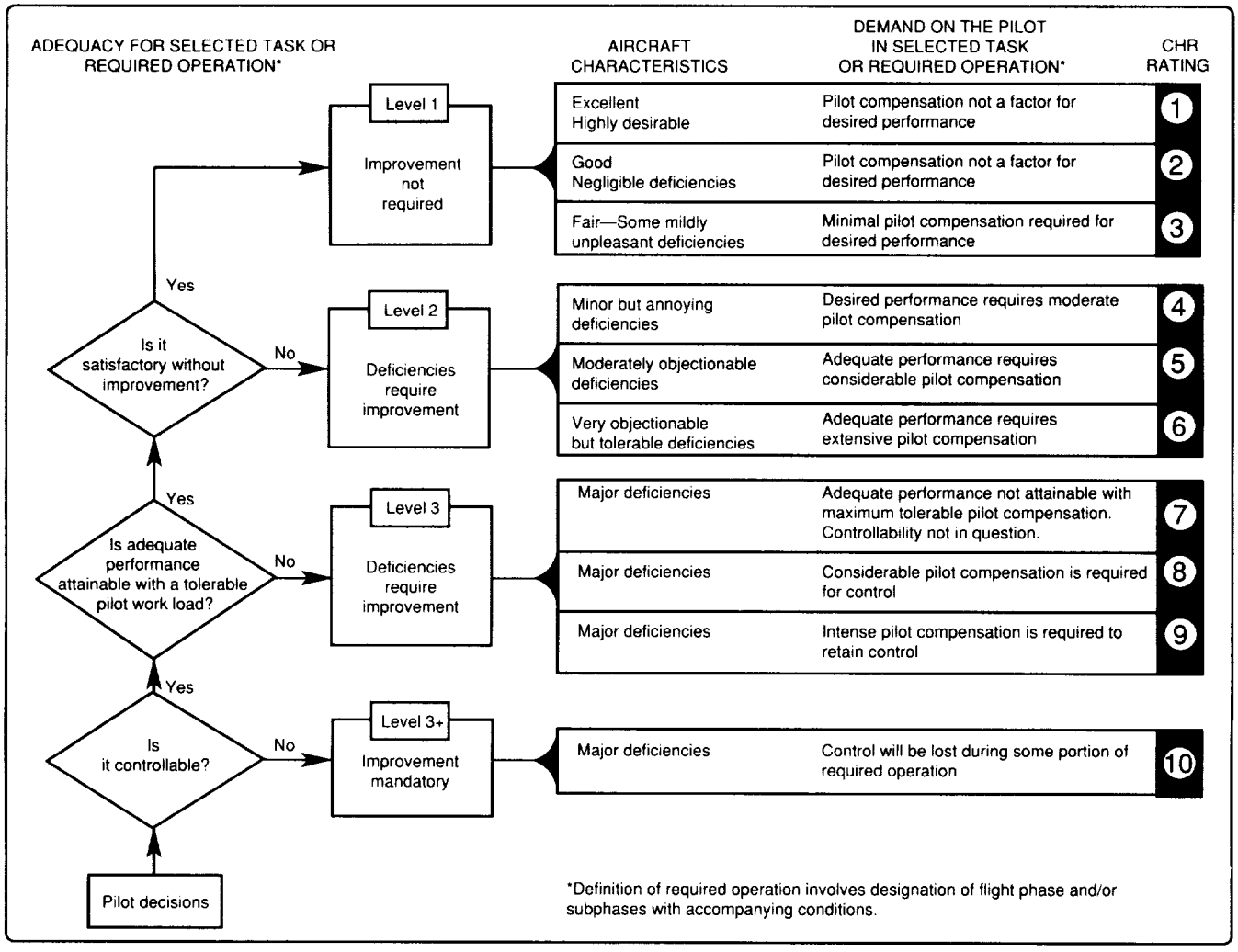

Figure 7. Pilot rating system (from ref. 6).

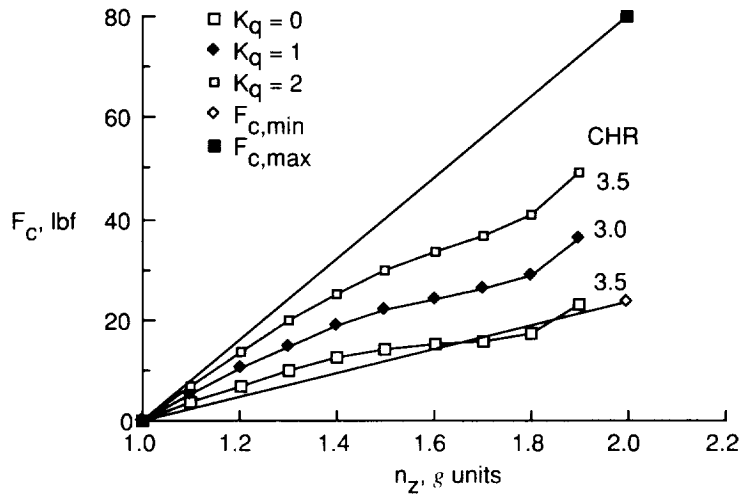

(a) Configurations 1, 2, and 3; c.g = $0.12\bar{c}$; SM = 33 percent.

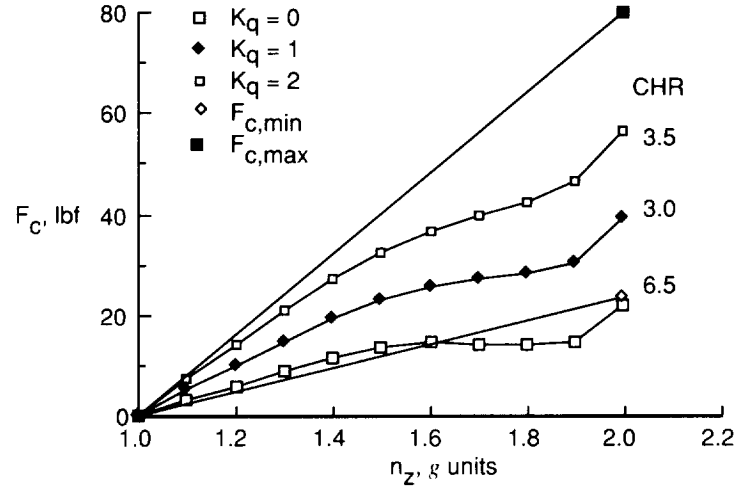

(b) Configurations 4, 5, and 6; c.g. = $0.25\bar{c}$; SM = 20 percent.

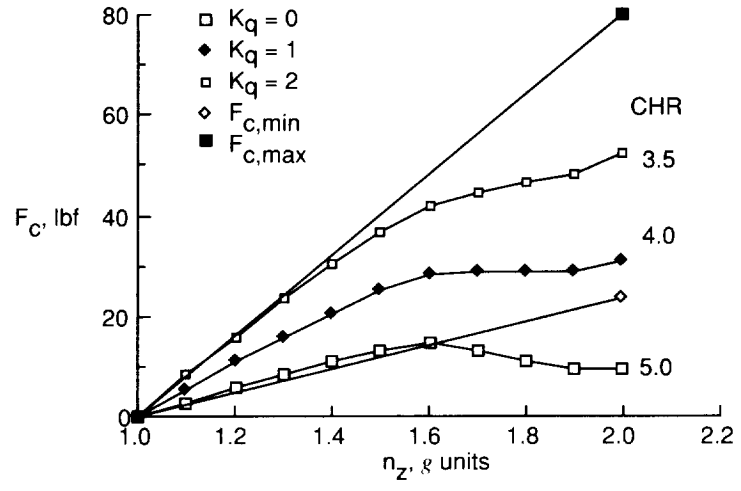

(c) Configurations 7, 8, and 9; c.g. = $0.35\bar{c}$; SM = 10 percent.

Figure 8. Effect of c.g. and K_q on F_c/n_z and on pilot rating.

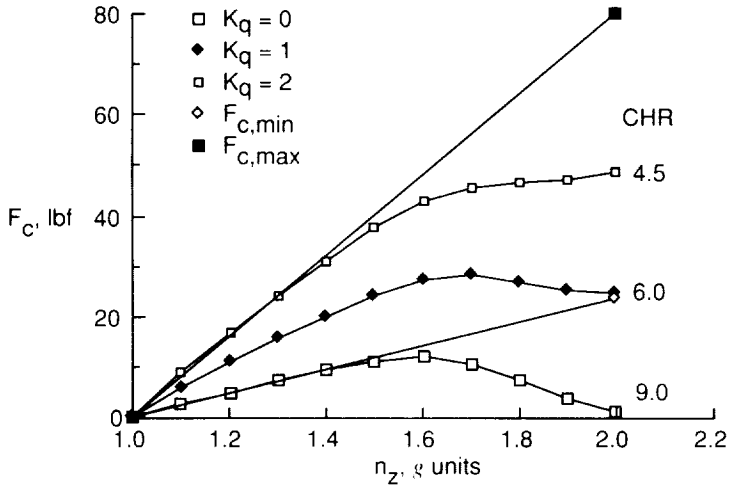

(d) Configurations 10, 11, and 12; c.g. = 0.40$\bar{c}$; SM = 5 percent.

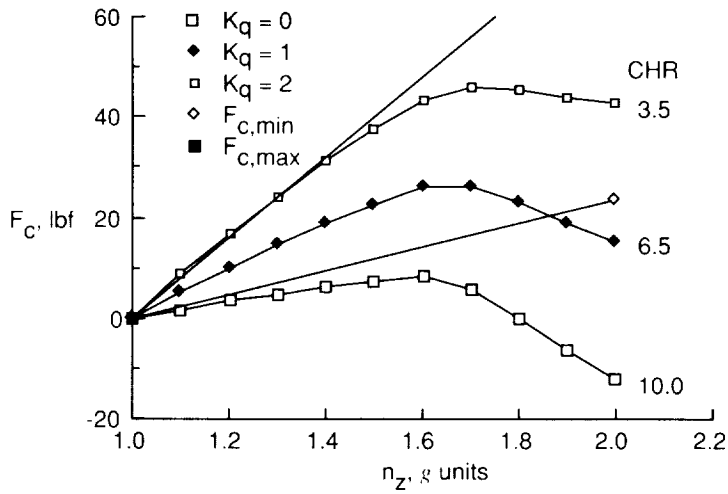

(e) Configurations 13, 14, and 15; c.g. = 0.45$\bar{c}$; SM = 0.

Figure 8. Continued.

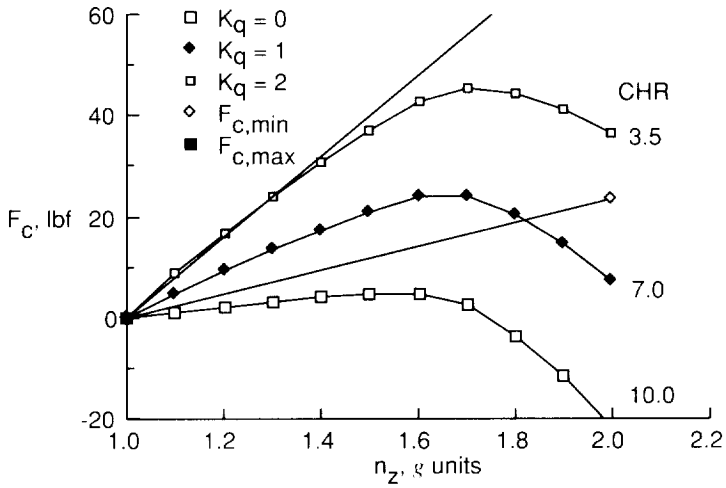

(f) Configurations 16, 17, and 18; c.g. = 0.47c; SM = −2 percent.

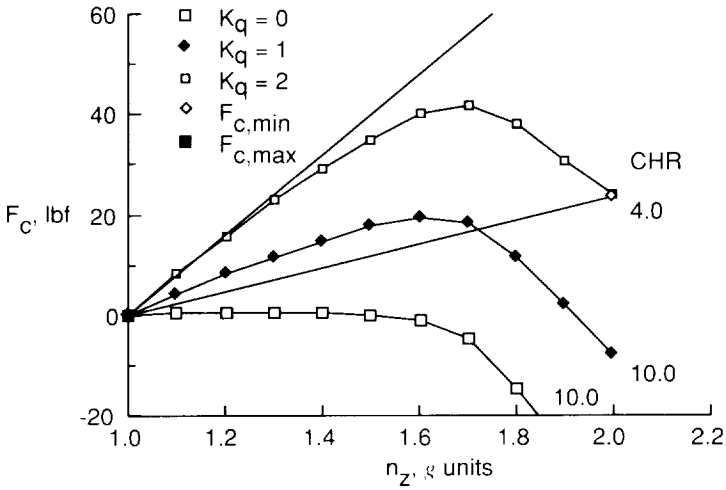

(g) Configurations 19, 20, and 21; c.g. = 0.50c; SM = −5 percent.

Figure 8. Concluded.

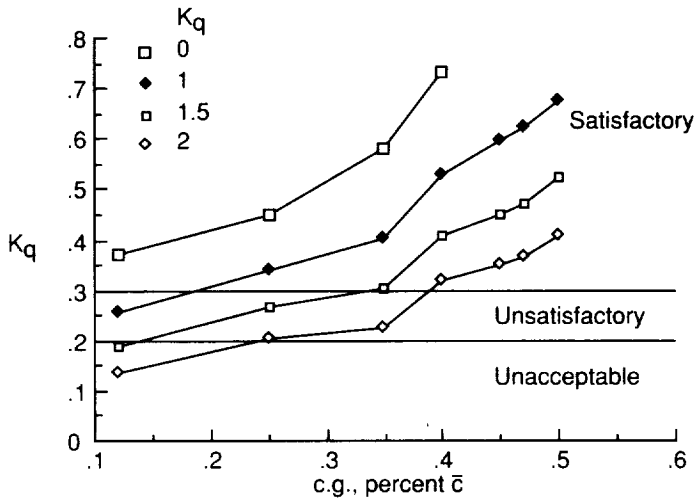

Figure 9. Effect of c.g. and K_q on short-period damping.

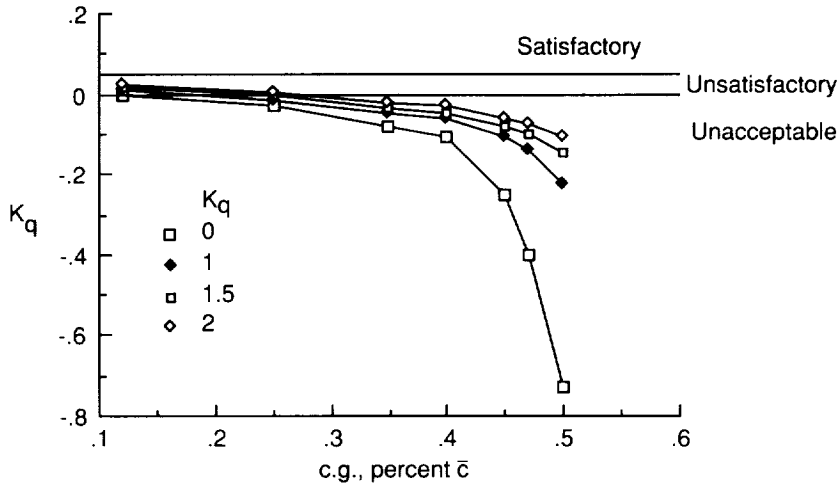

Figure 10. Effect of c.g. and K_q on phugoid damping.

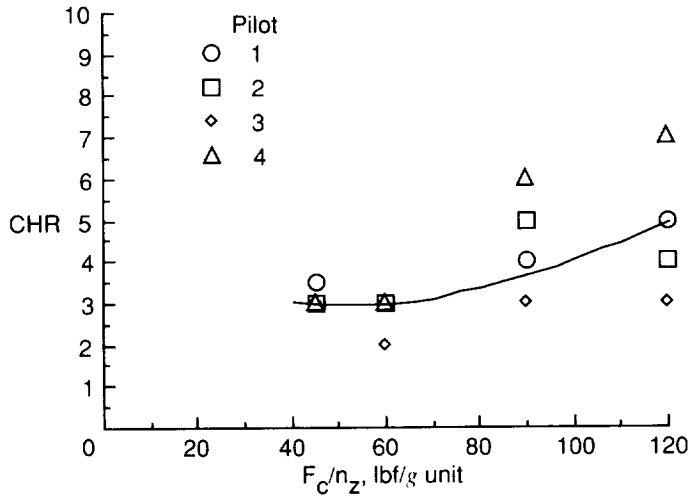

(a) Configurations 67 through 70; c.g. $= 0.40\bar{c}$; SM = 5 percent.

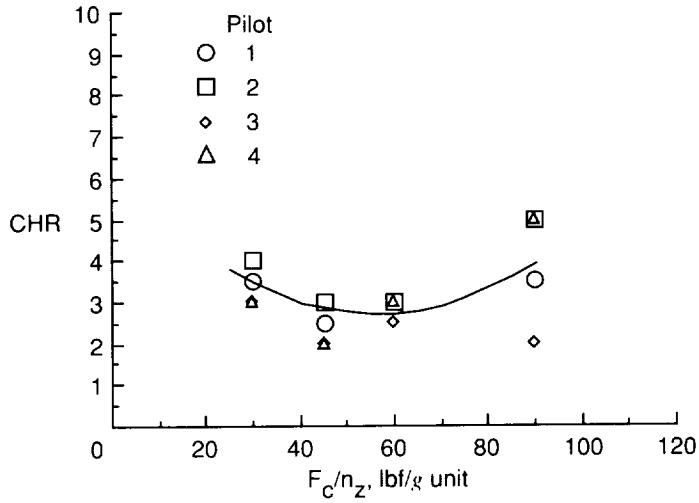

(b) Configurations 71 through 74; c.g. $= 0.45\bar{c}$; SM = 0.

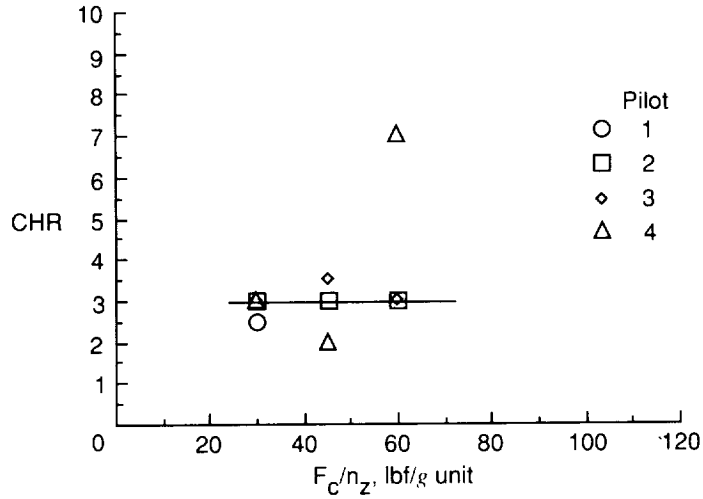

(c) Configurations 79 through 81; c.g. $= 0.50\bar{c}$; SM $= -5$ percent.

Figure 11. Pilot ratings for various levels of maneuver stability. Variable F_c/δ_c; $\delta_H/\delta_c = -1.0°$/in.

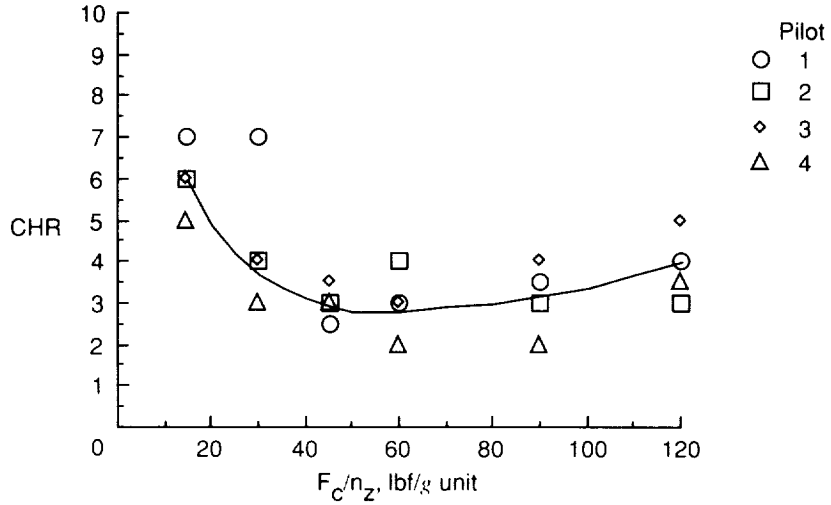

(a) Configurations 34 through 39; c.g. $= 0.40\bar{c}$; SM = 5 percent.

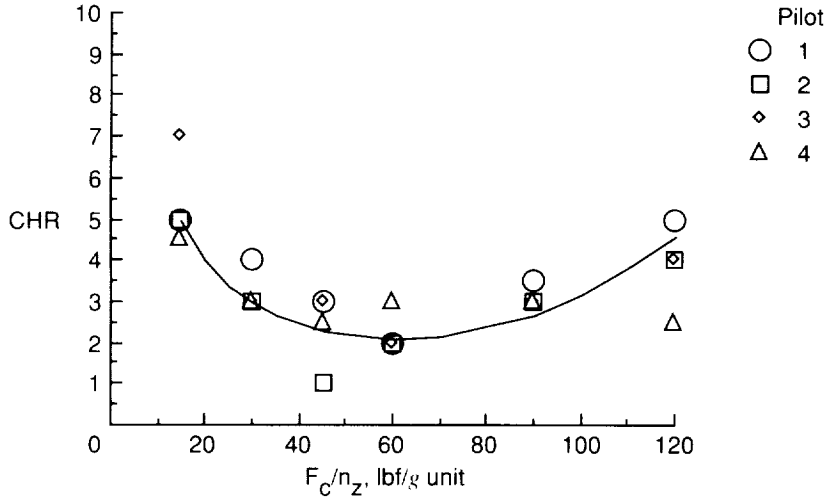

(b) Configurations 40 through 45; c.g. $= 0.45\bar{c}$; SM = 0.

Figure 12. Pilot ratings for various levels of linear maneuver stability. Variable δ_H/δ_c; $F_c/\delta_c = 15.77$ lbf/in.

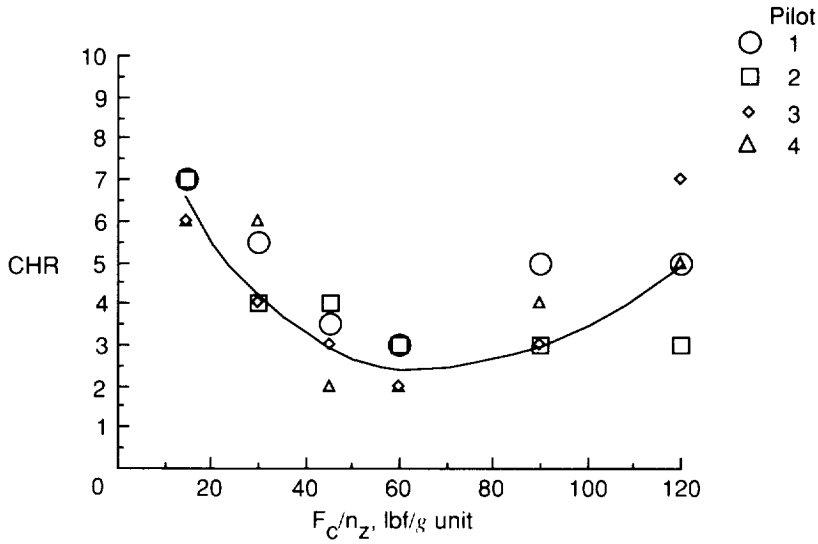

(c) Configurations 52 through 57; c.g. = 0.50$\bar{c}$; SM = −5 percent.

Figure 12. Concluded.

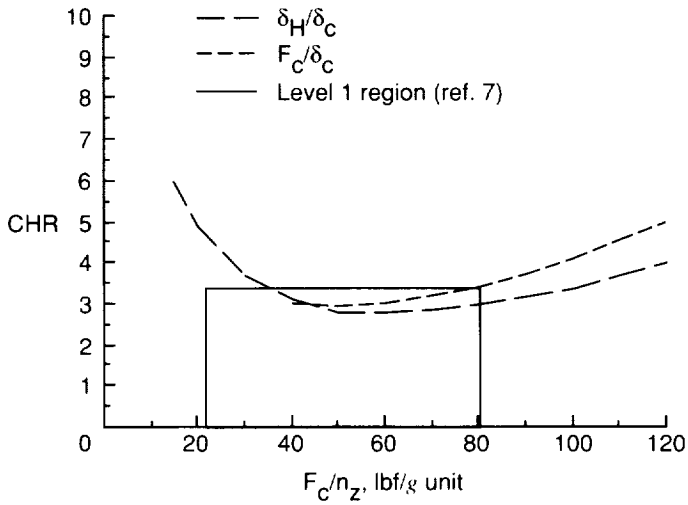

(a) c.g. $= 0.40\bar{c}$; SM $= 5$ percent.

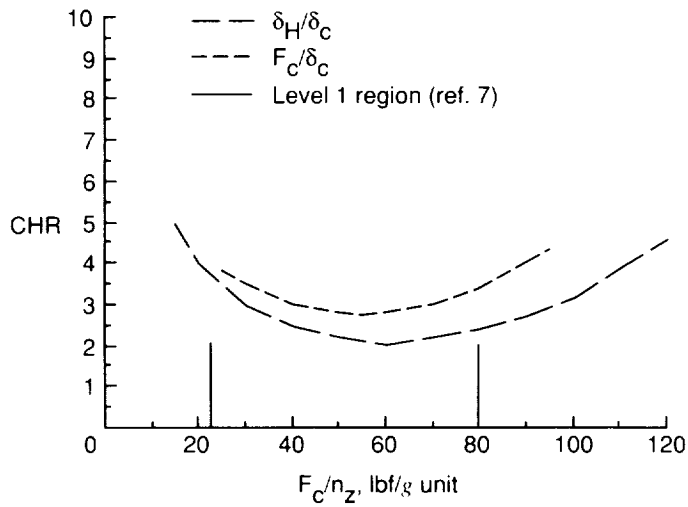

(b) c.g. $= 0.45\bar{c}$; SM $= 0$.

Figure 13. Pilot ratings for techniques used to maintain linear maneuver stability.

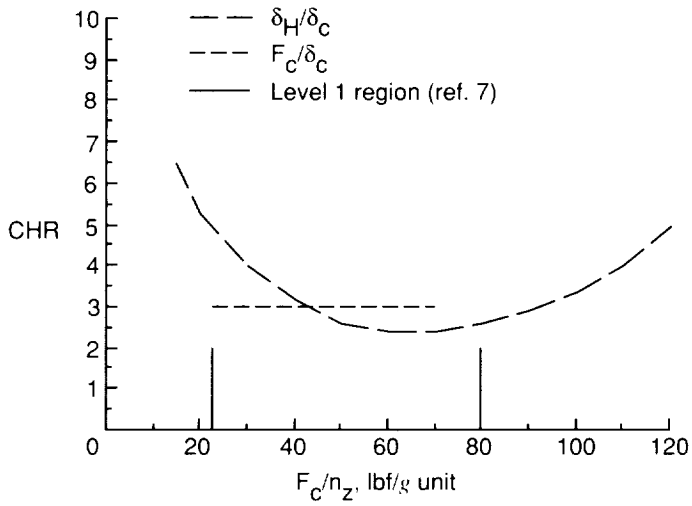

(c) c.g. $= 0.50\bar{c}$; SM $= -5$ percent.

Figure 13. Concluded.

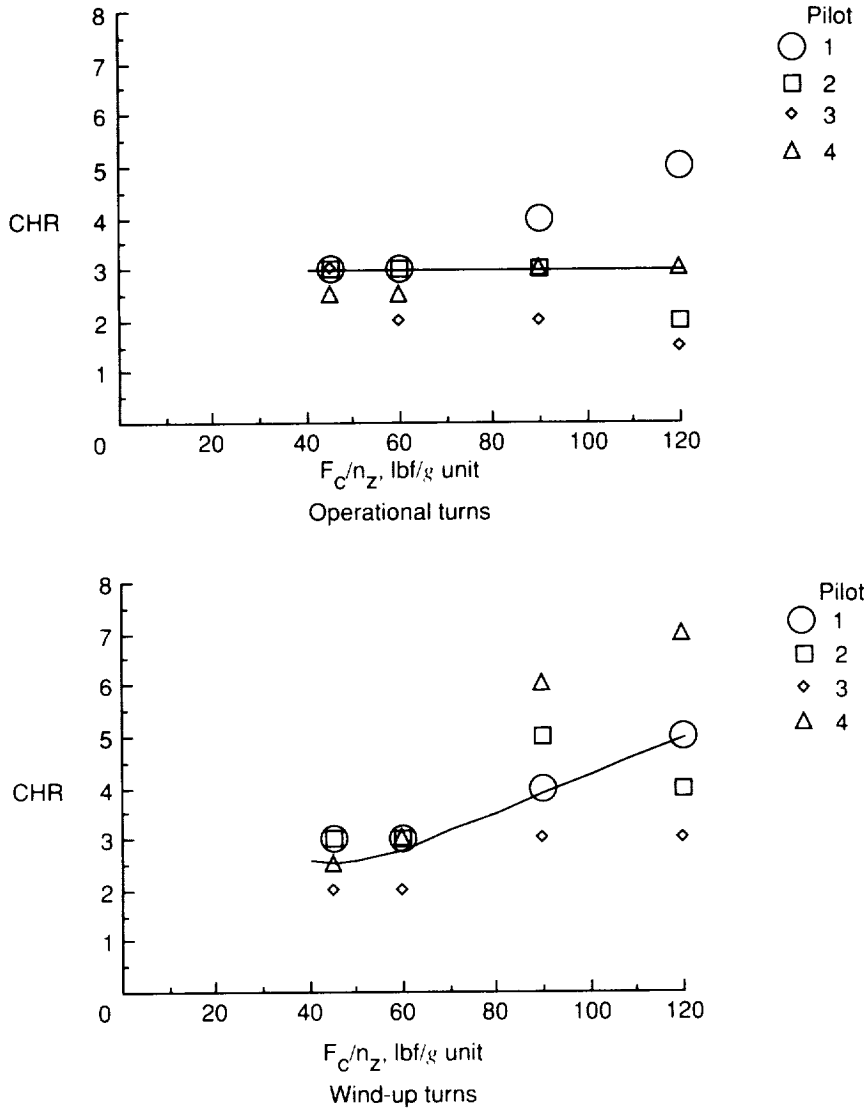

(a) Configurations 67 through 70; c.g. $= 0.40\bar{c}$; SM = 5 percent.

Figure 14. Effect of magnitude of linear maneuver stability on pilot rating for operational and wind-up turns. Variable F_c/δ_c; $\delta_H/\delta_c = -1.0°/\text{in}$.

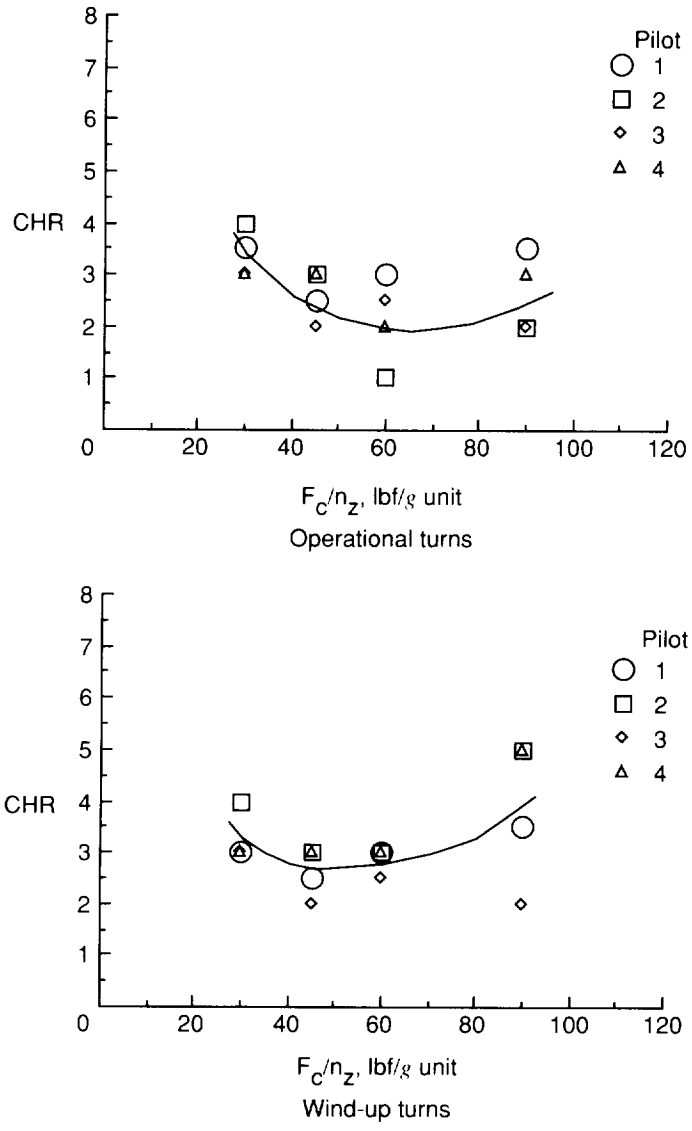

(b) Configurations 71 through 74; c.g. $= 0.45\bar{c}$; SM $= 0$.

Figure 14. Continued.

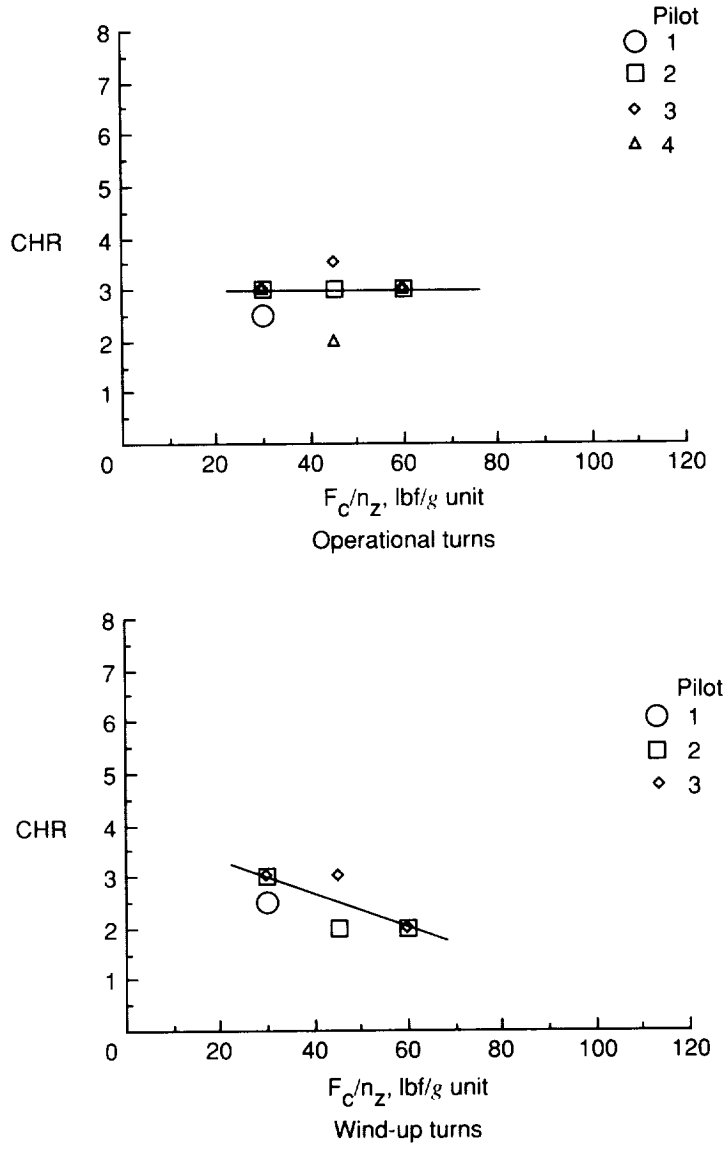

(c) Configurations 79 through 81; c.g. $= 0.50\bar{c}$; SM $= -5$ percent.

Figure 14. Concluded.

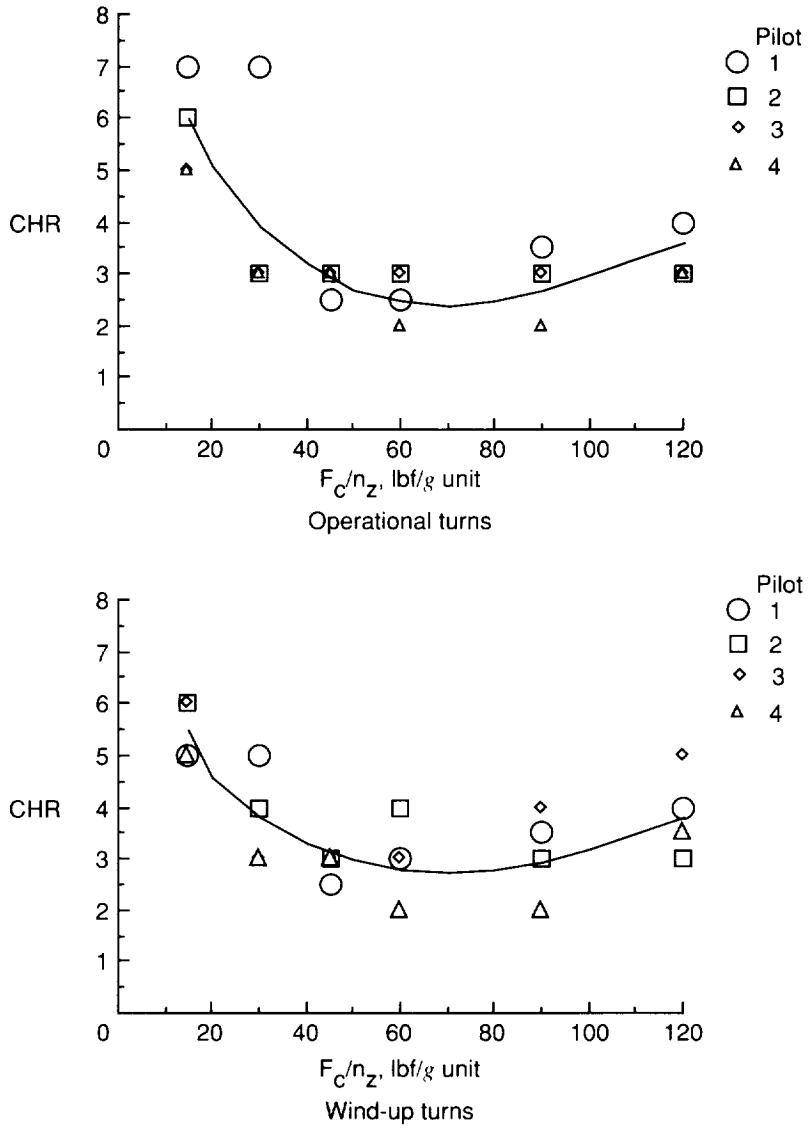

(a) Configurations 34 through 39; c.g. = $0.40\bar{c}$; SM = 5 percent.

Figure 15. Effect of magnitude of linear maneuver stability on pilot opinion for operational and wind-up turns. Variable δ_H/δ_c; F_c/δ_c = 15.77 lbf/in.

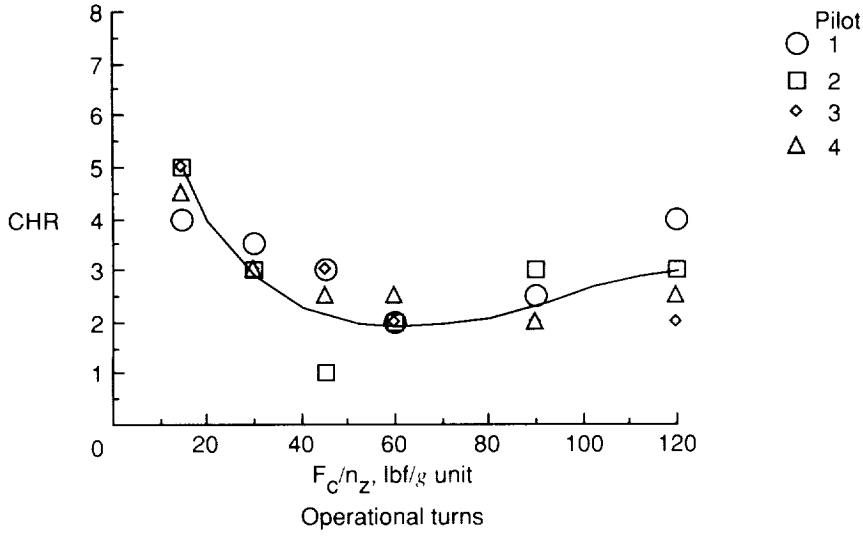

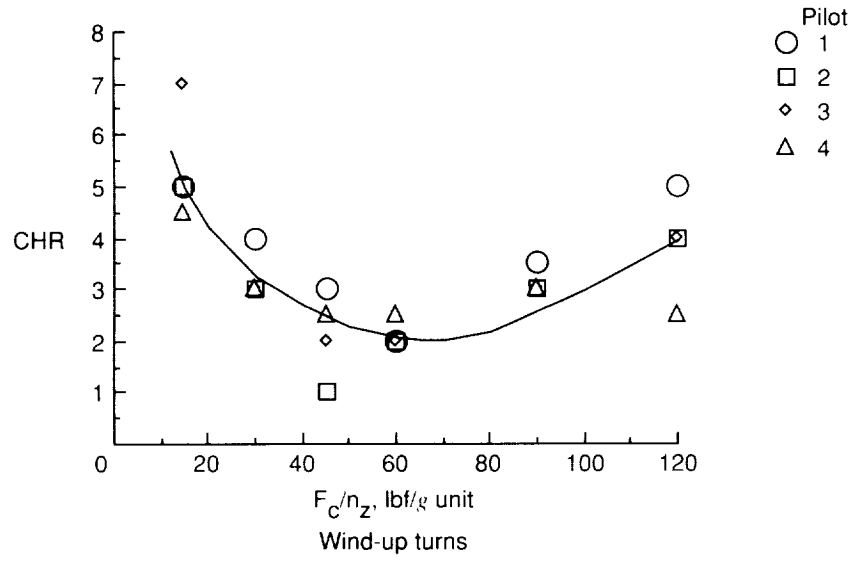

(b) Configurations 40 through 45; c.g. $= 0.45\bar{c}$; SM $= 0$.

Figure 15. Continued.

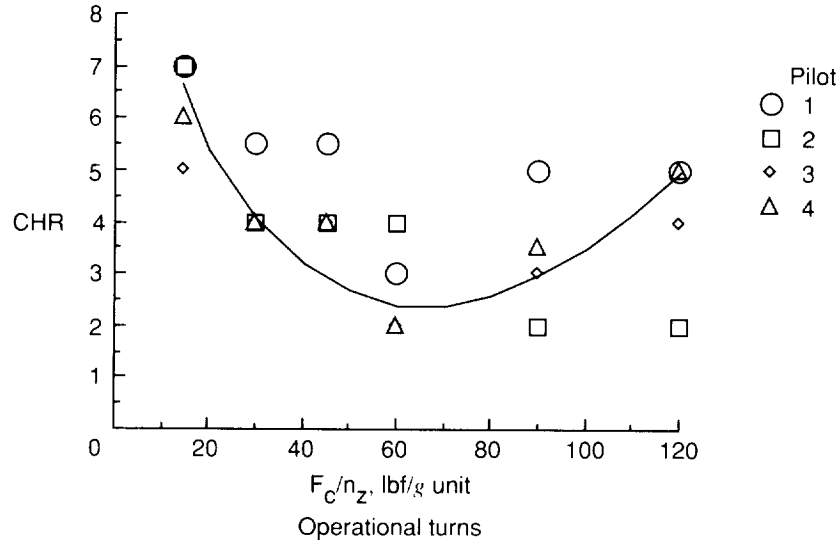

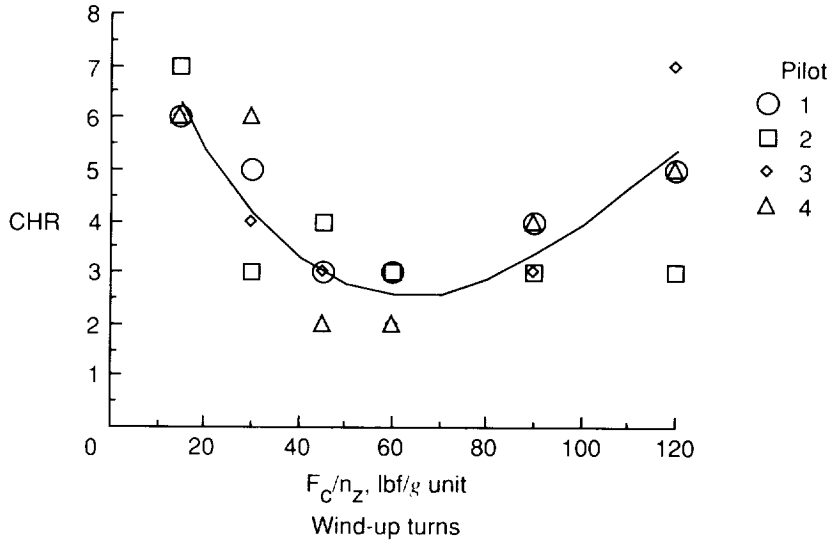

(c) Configurations 52 through 57; c.g. $= 0.50\bar{c}$; SM $= -5$ percent.

Figure 15. Concluded.

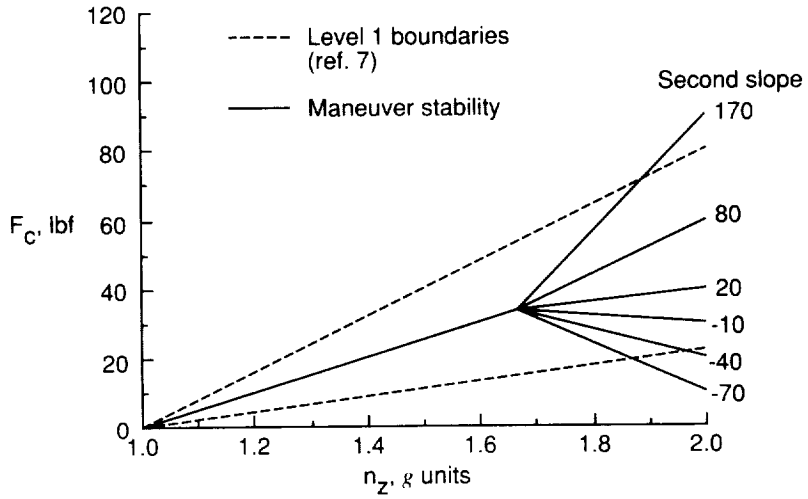

Figure 16. Maneuver stability characteristics with single break at 1.667g.

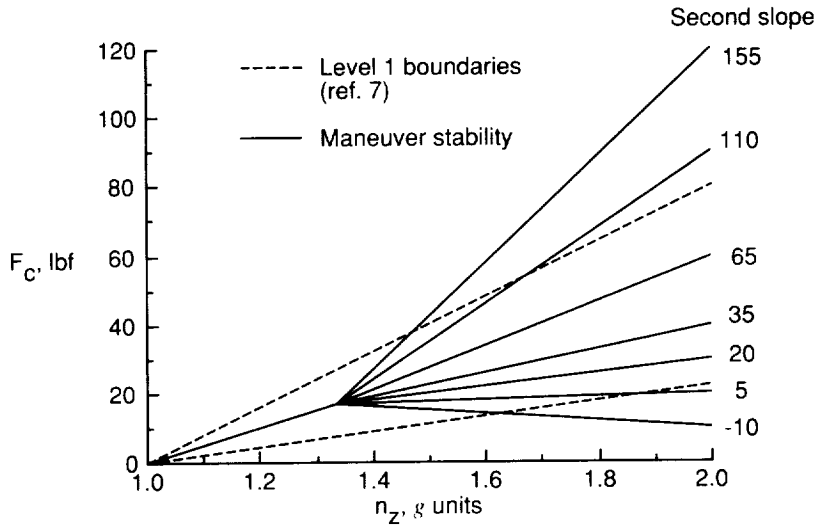

Figure 17. Maneuver stability characteristics with single break at 1.333g.

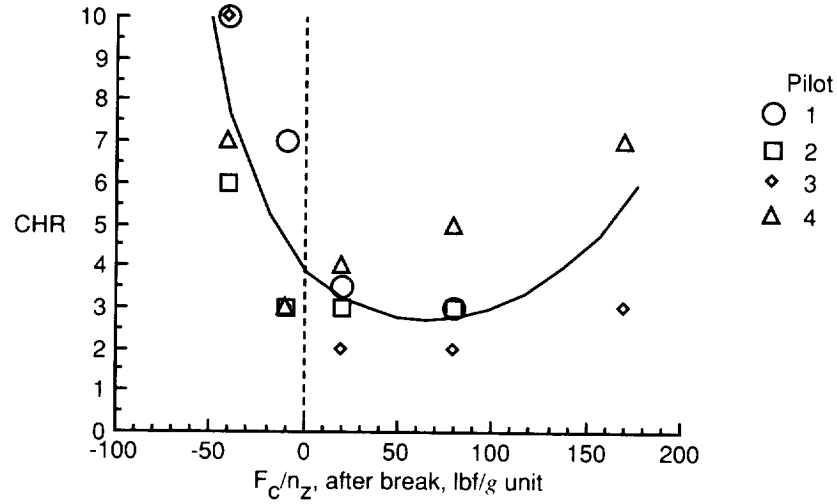

(a) Configurations 100 through 104; c.g. $= 0.40\bar{c}$; SM = 5 percent.

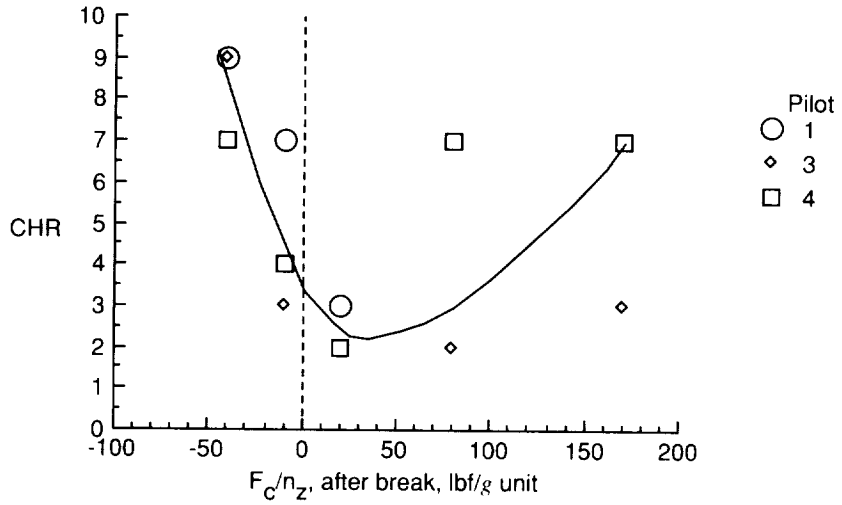

(b) Configurations 105 through 109; c.g. $= 0.45\bar{c}$; SM = 0.

Figure 18. Effect of single break in maneuver stability on pilot opinion. Break at $n_z = 1.667g$; variable F_c/δ_c; $\delta_H/\delta_c = -1.0°/\text{in}$.

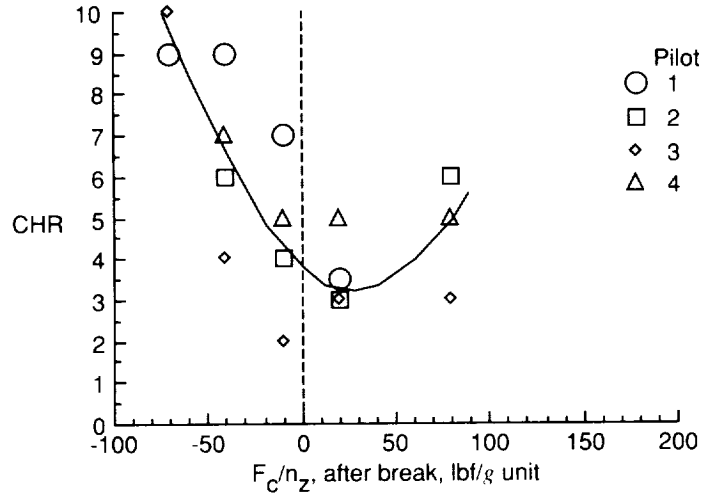

(c) Configurations 110 through 114; c.g. $= 0.50\bar{c}$; SM $= -5$ percent.

Figure 18. Concluded.

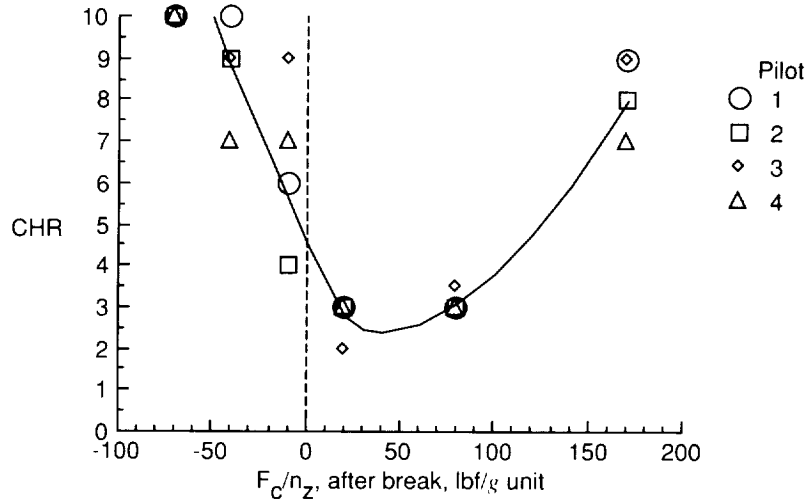

(a) Configurations 82 through 87; c.g. $= 0.40\bar{c}$; SM = 5 percent.

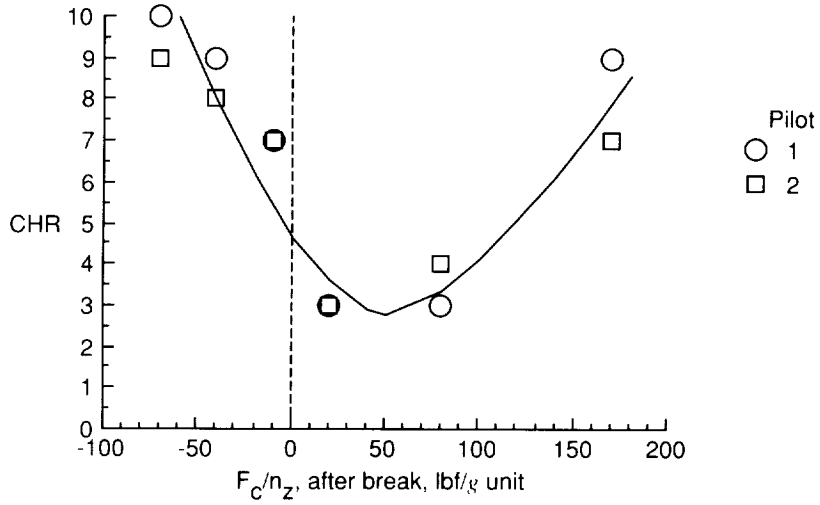

(b) Configurations 88 through 93; c.g. $= 0.45\bar{c}$; SM = 0.

Figure 19. Effect of single break in maneuver stability on pilot opinion. Break at $n_z = 1.667g$; variable δ_H/δ_c; $F_c/\delta_c = 15.77$ lbf/in.

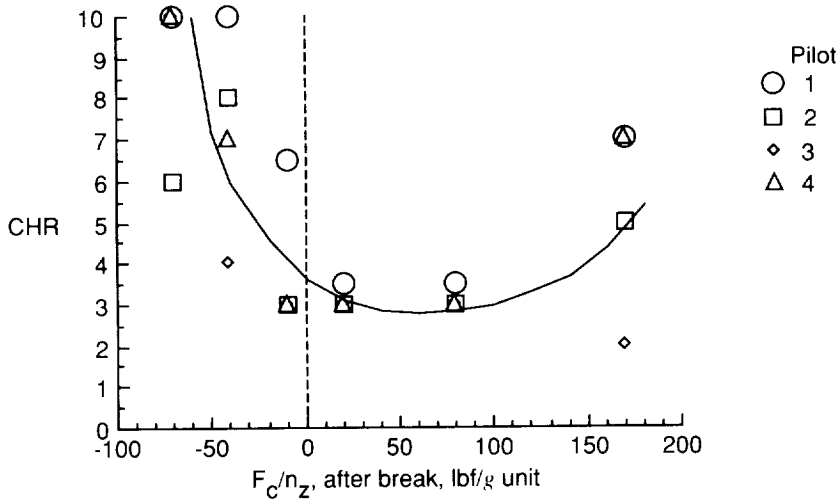

(c) Configurations 94 through 99; c.g. $= 0.50\bar{c}$; SM $= -5$ percent.

Figure 19. Concluded.

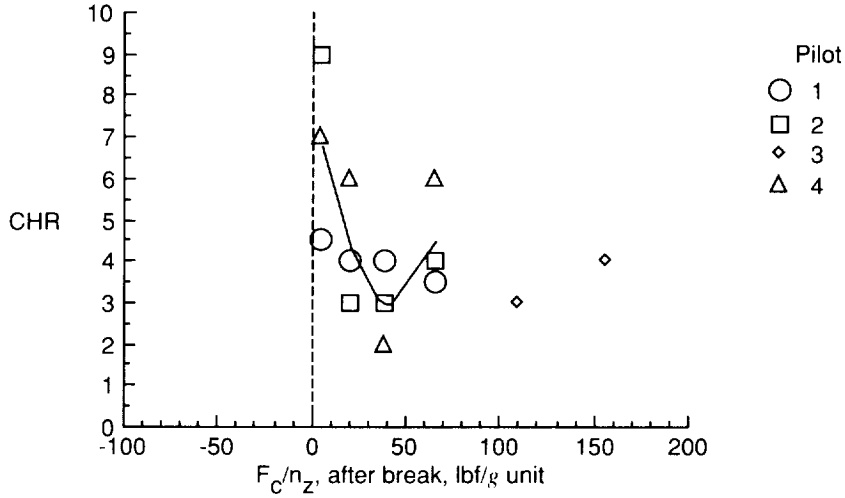

(a) Configurations 136 through 141; c.g. $= 0.40\bar{c}$; SM $= 5$ percent.

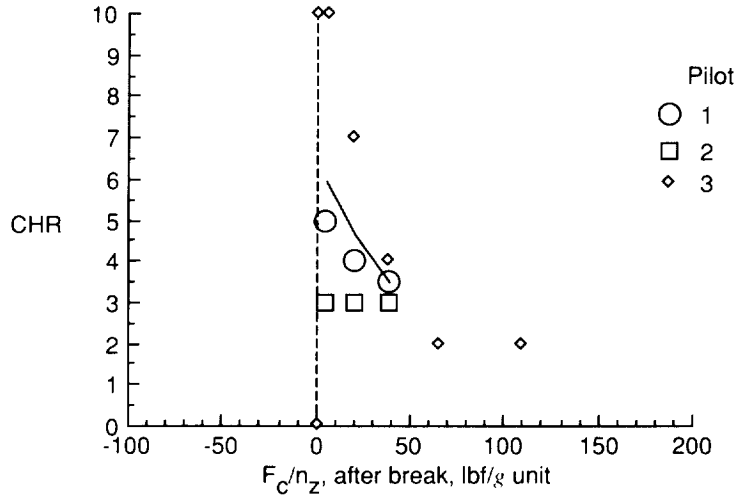

(b) Configurations 142 through 146; c.g. $= 0.45\bar{c}$; SM $= 0$.

Figure 20. Effect of single break in maneuver stability on pilot opinion. Break at $n_z = 1.333g$; variable F_c/δ_c; $\delta_H/\delta_c = -1.0°/\text{in}$.

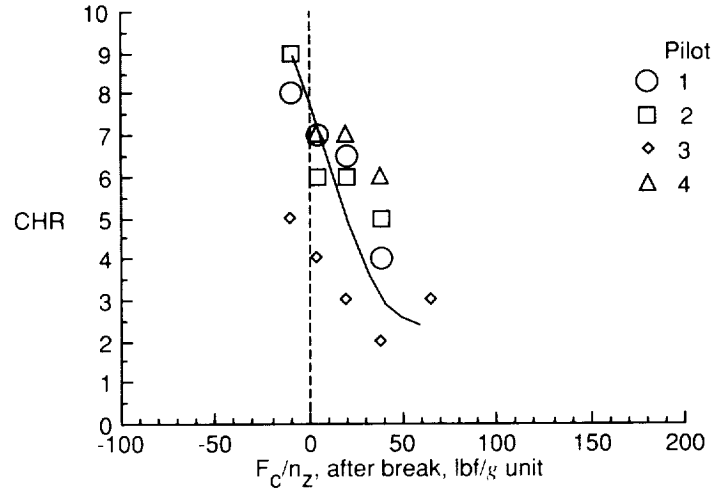

(c) Configurations 147 through 151; c.g. = $0.50\bar{c}$; SM = -5 percent.

Figure 20. Concluded.

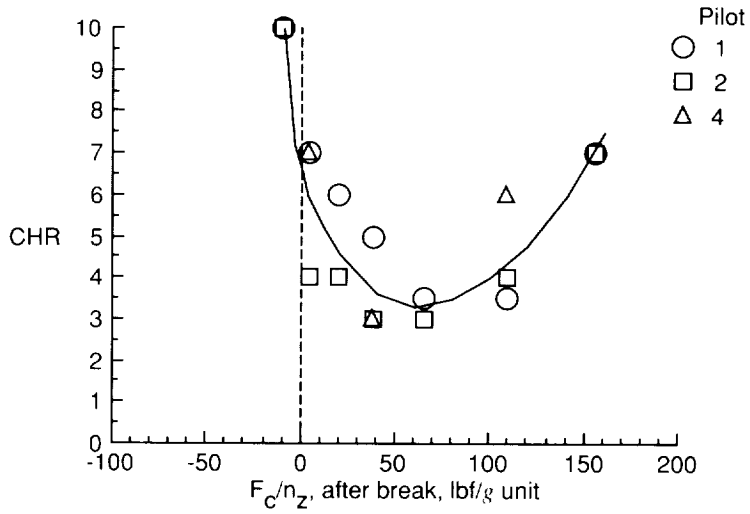

(a) Configurations 115 through 121; c.g. $= 0.40\bar{c}$; SM = 5 percent.

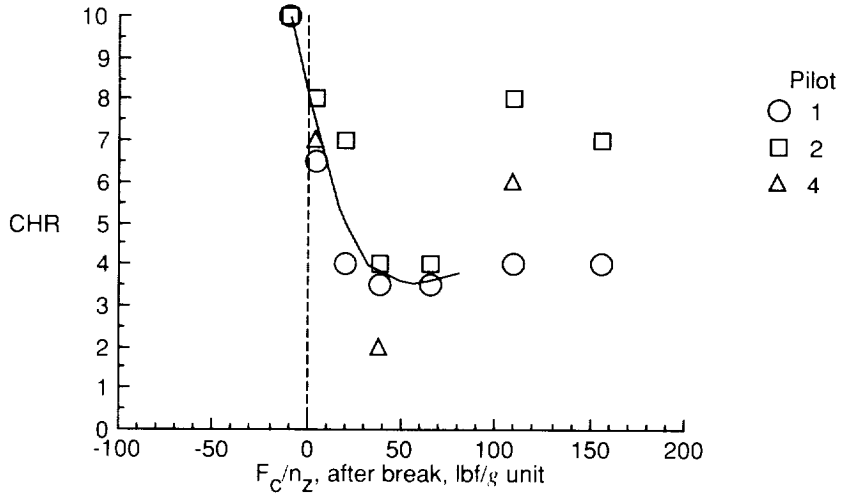

(b) Configurations 122 through 128; c.g. $= 0.45\bar{c}$; SM = 0.

Figure 21. Effect of single break in maneuver stability on pilot opinion. Break at $n_z = 1.333g$; variable δ_H/δ_c; $F_c/\delta_c = 15.77$ lbf/in.

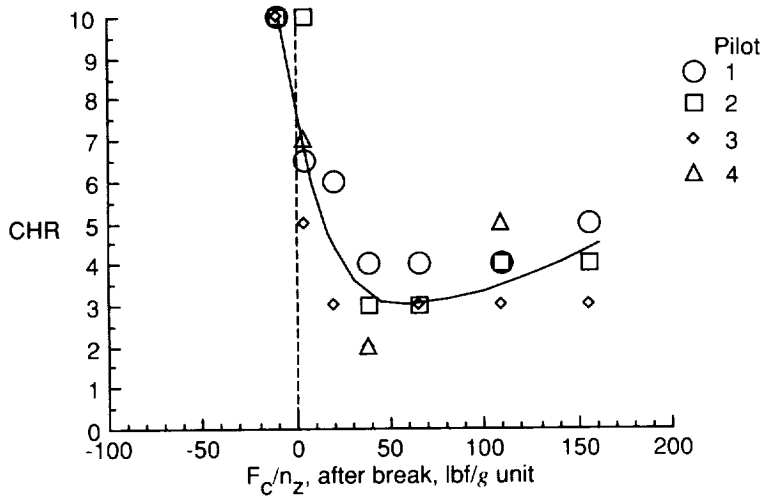

(c) Configurations 129 through 135; c.g. = $0.50\bar{c}$; SM = -5 percent.

Figure 21. Concluded.

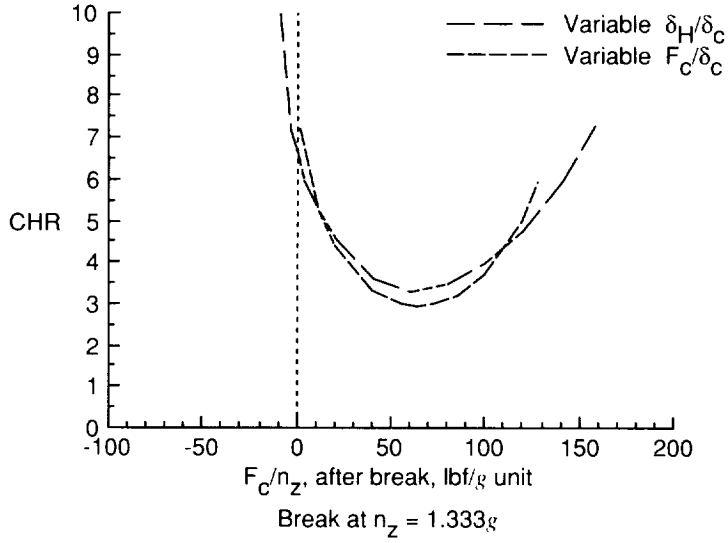

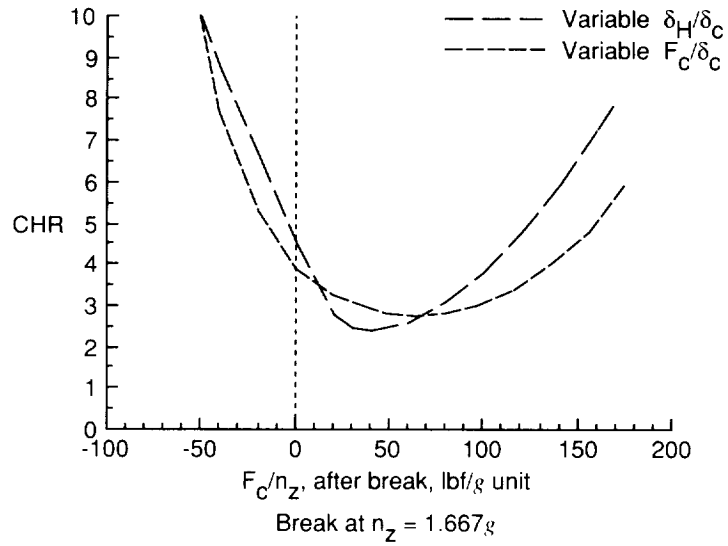

(a) c.g. $= 0.40\bar{c}$; SM $= 5$ percent.

Figure 22. Trends for methods used (variable δ_H/δ_c of F_c/δ_c) to adjust maneuver stability characteristics.

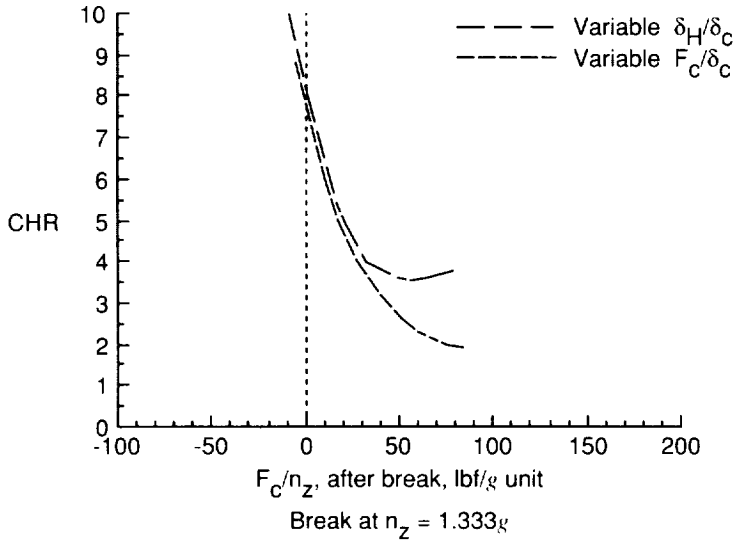

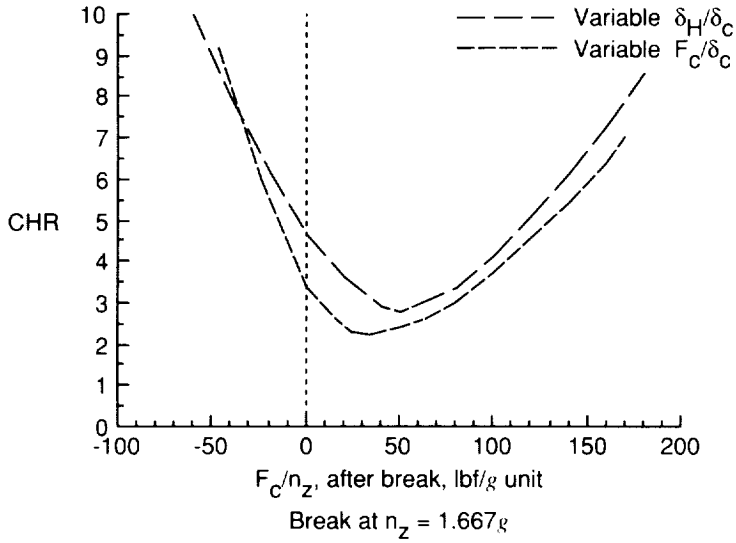

(b) c.g. $= 0.45\bar{c}$; SM $= 0$.

Figure 22. Continued.

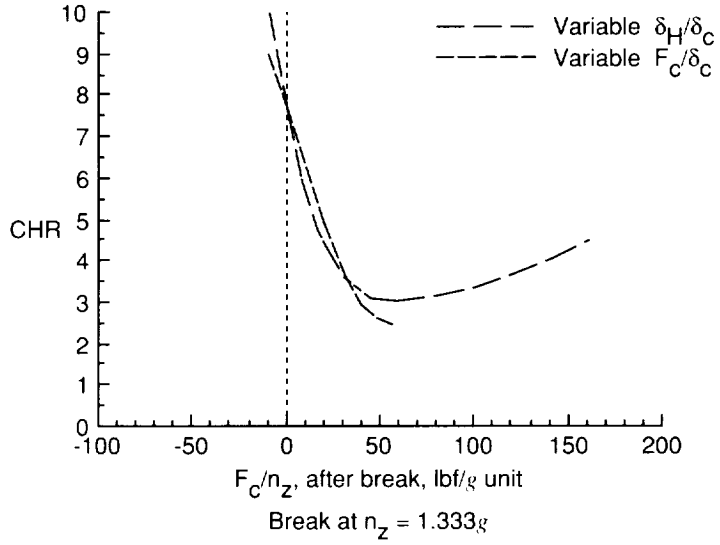

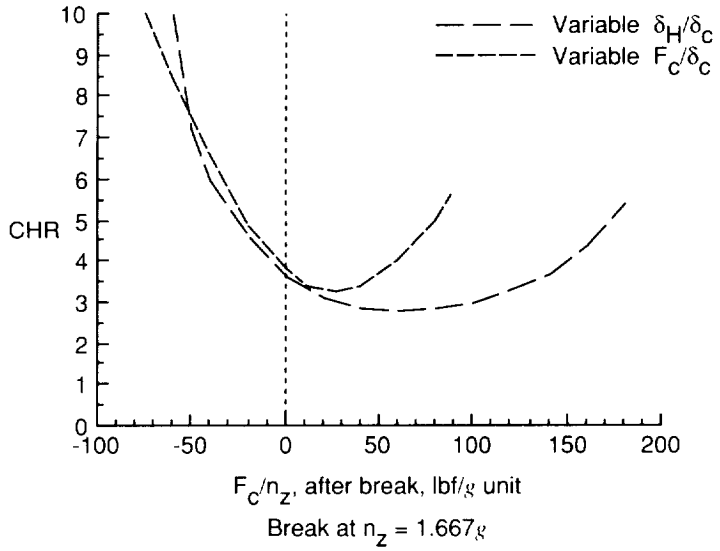

(c) c.g. $= 0.50\bar{c}$; SM $= -5$ percent.

Figure 22. Concluded.

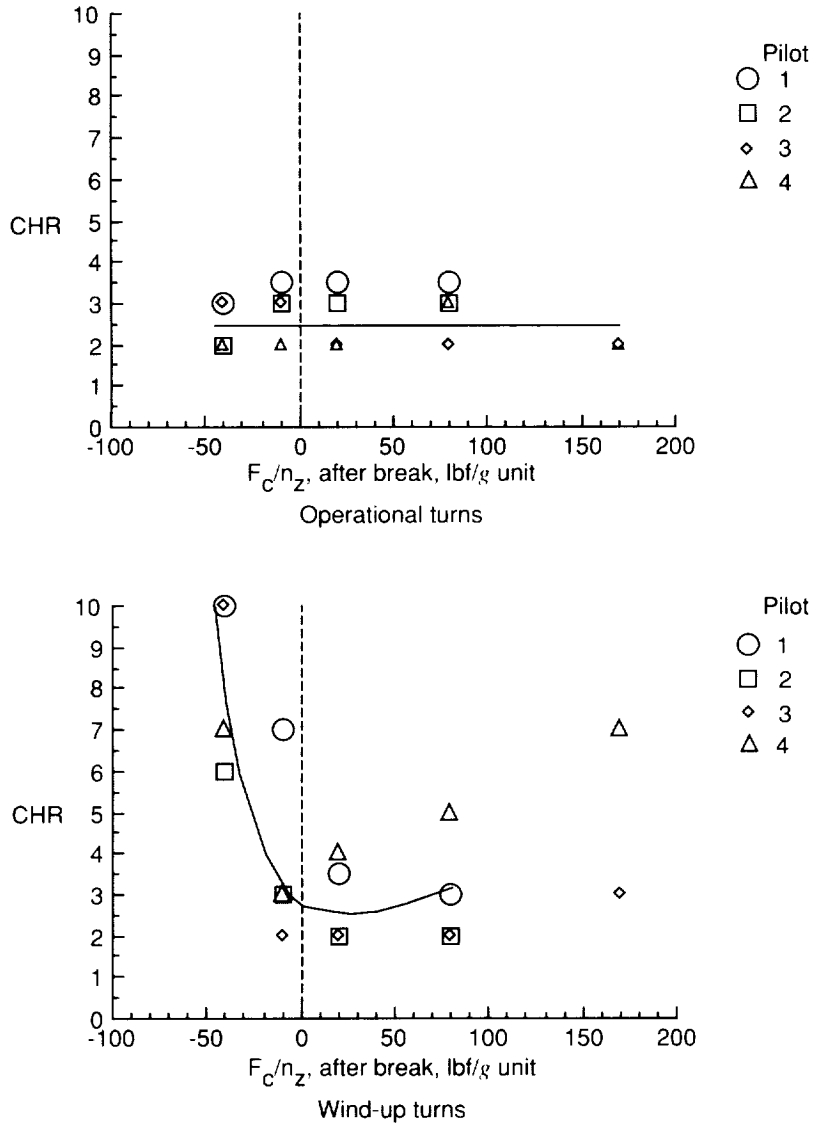

(a) Configurations 100 through 104; c.g. = $0.40\bar{c}$; SM = 5 percent.

Figure 23. Effect of single break in maneuver stability curve and c.g. location on individual pilot ratings. Initial slope = 50 lbf/g; break at $n_z = 1.667g$; variable F_c/δ_c; $\delta_H/\delta_c = -1°$/in.

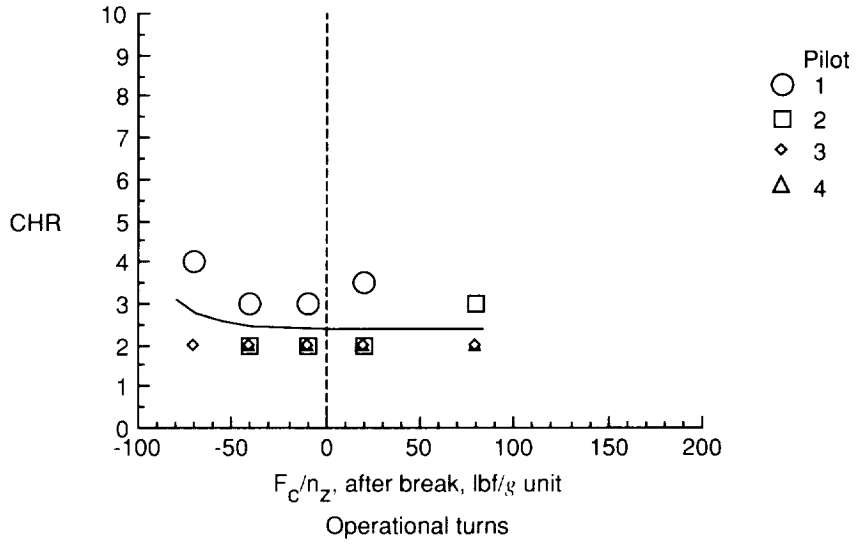

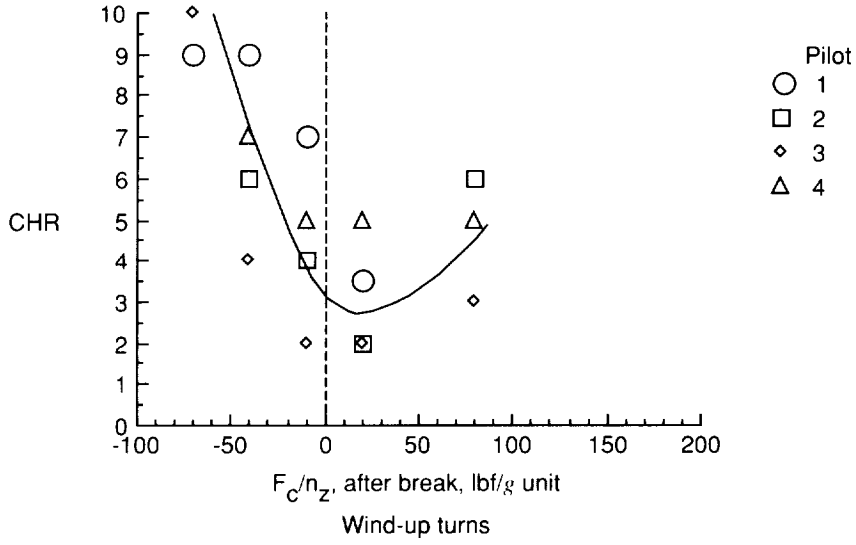

(b) Configurations 110 through 114; c.g. = 0.50$\bar{c}$; SM = −5 percent.

Figure 23. Concluded.

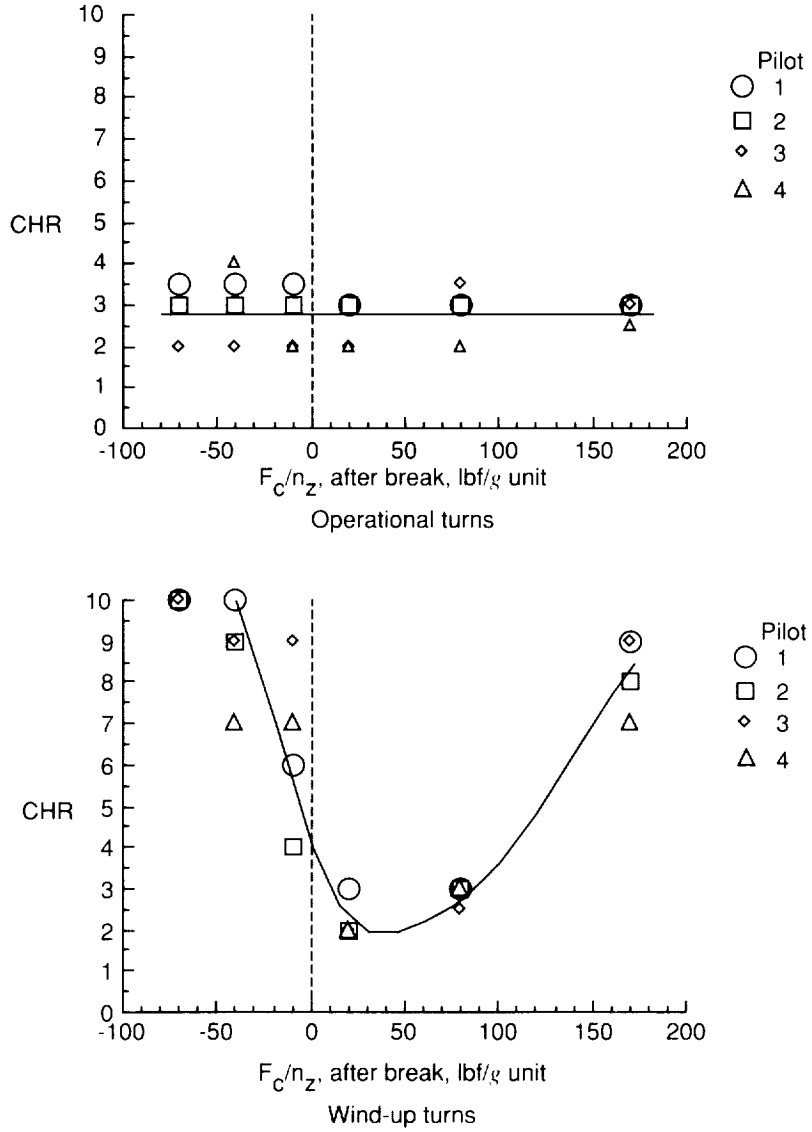

(a) Configurations 82 through 87; c.g. $= 0.40\bar{c}$; SM = 5 percent.

Figure 24. Effect of single break in maneuver stability curve and c.g. location on individual pilot ratings. Initial slope = 50 lbf/g; break at $n_z = 1.667g$; variable δ_H/δ_c; $F_c/\delta_c = 15.77$ lbf/in.

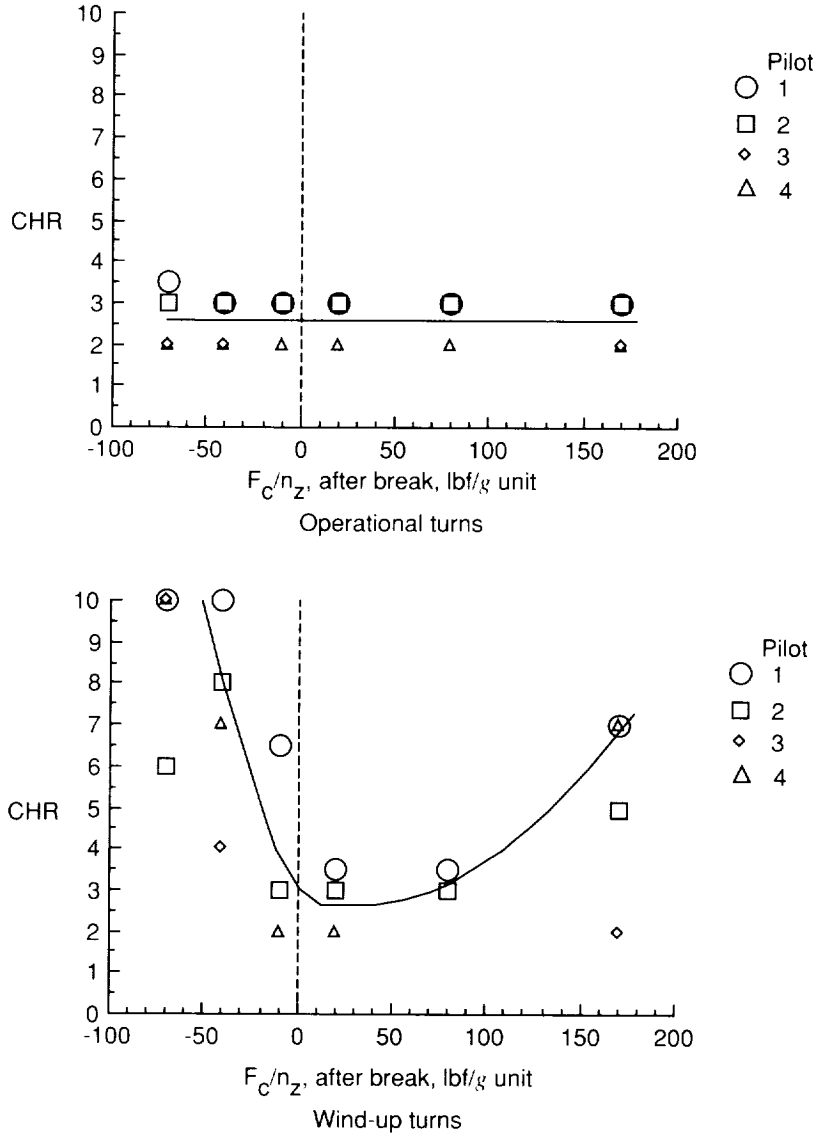

(b) Configurations 94 through 99; c.g. $= 0.50\bar{c}$; SM $= -5$ percent.

Figure 24. Concluded.

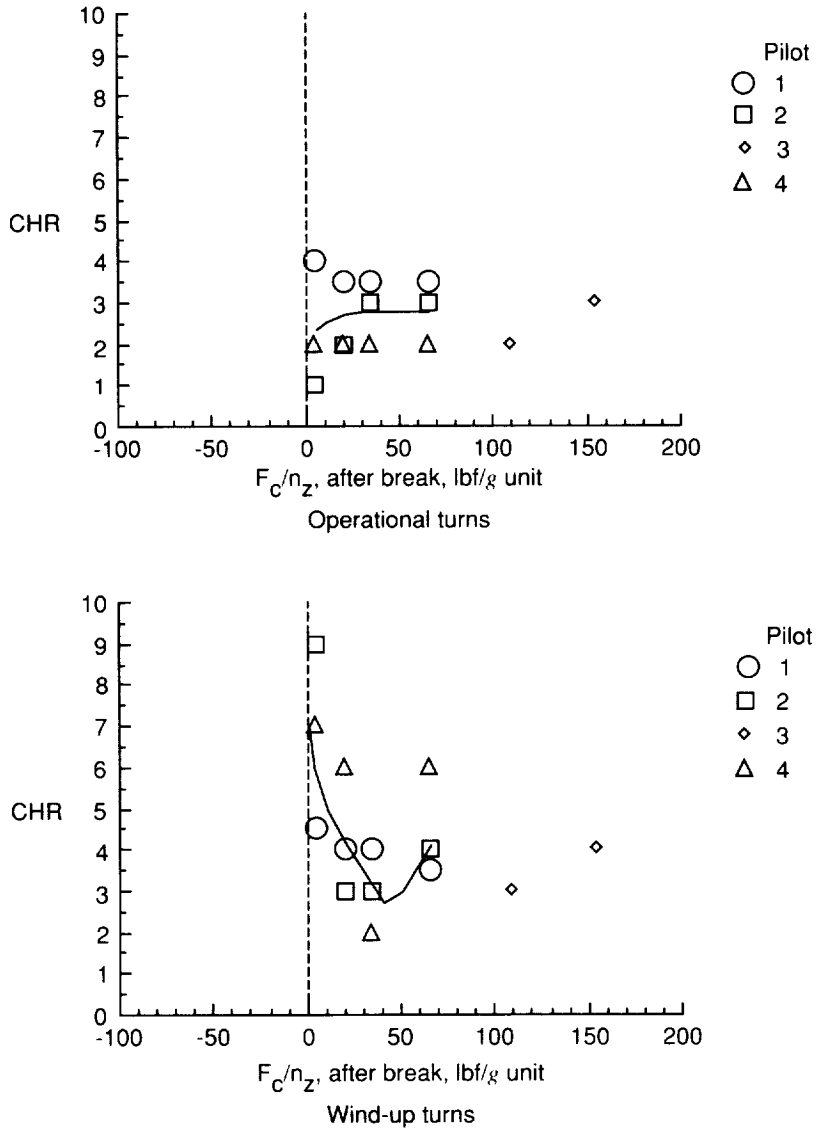

(a) Configurations 136 through 141; c.g. $= 0.40\bar{c}$; SM = 5 percent.

Figure 25. Effect of single break in maneuver stability curve and c.g. location on individual pilot ratings. Initial slope = 50 lbf/g; break at $n_z = 1.333g$; variable F_c/δ_c; $\delta_H/\delta_c = -1°$/in.

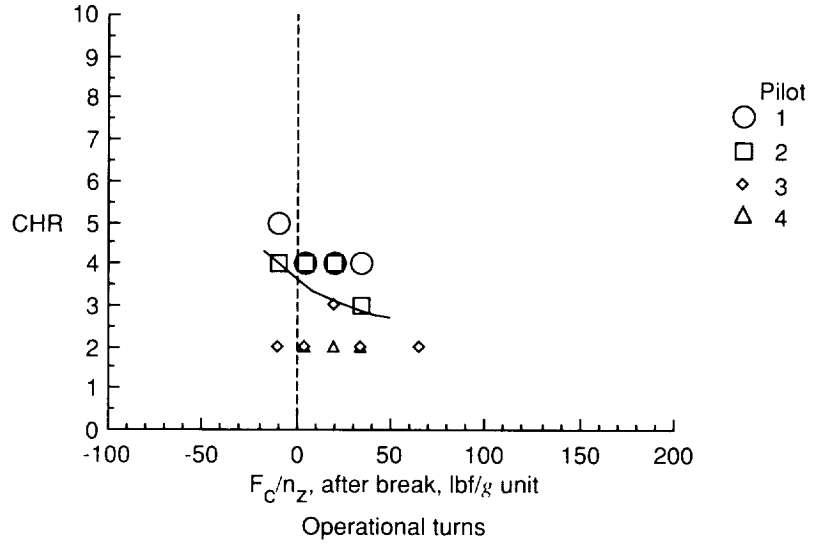

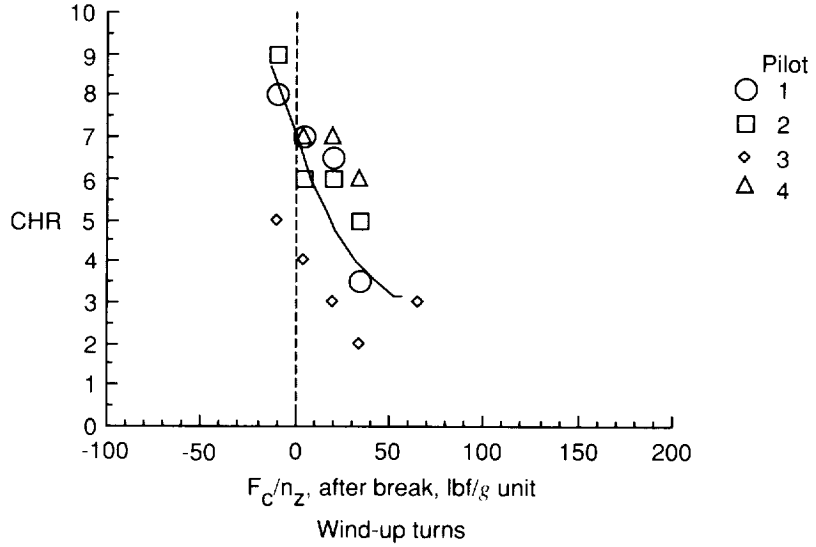

(b) Configurations 147 through 151; c.g. $= 0.50\bar{c}$; SM $= -5$ percent.

Figure 25. Concluded.

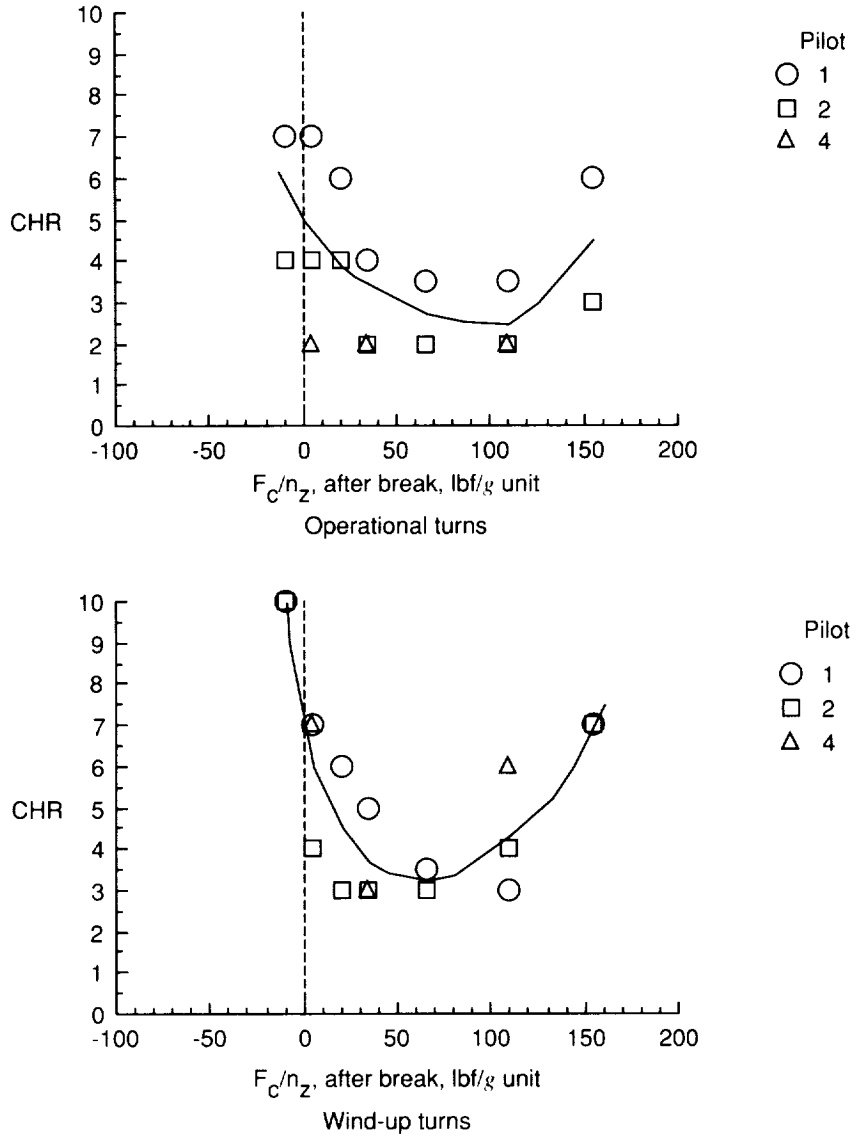

(a) Configurations 115 through 121; c.g. $= 0.40\bar{c}$; SM = 5 percent.

Figure 26. Effect of single break in maneuver stability curve and c.g. location on individual pilot ratings. Initial slope = 50 lbf/g; break at $n_z = 1.333g$; variable δ_H/δ_c; $F_c/\delta_c = 15.77$ lbf/in.

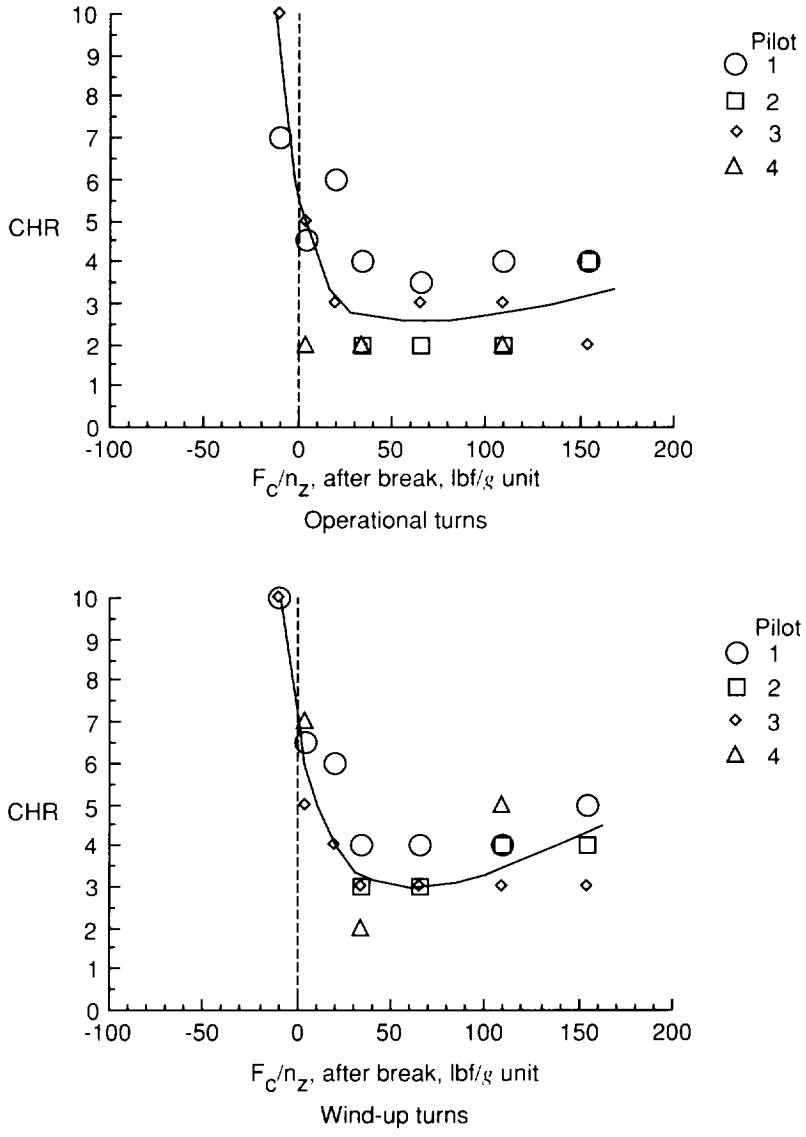

(b) Configurations 129 through 135; c.g. $= 0.50\bar{c}$; SM $= -5$ percent.

Figure 26. Concluded.

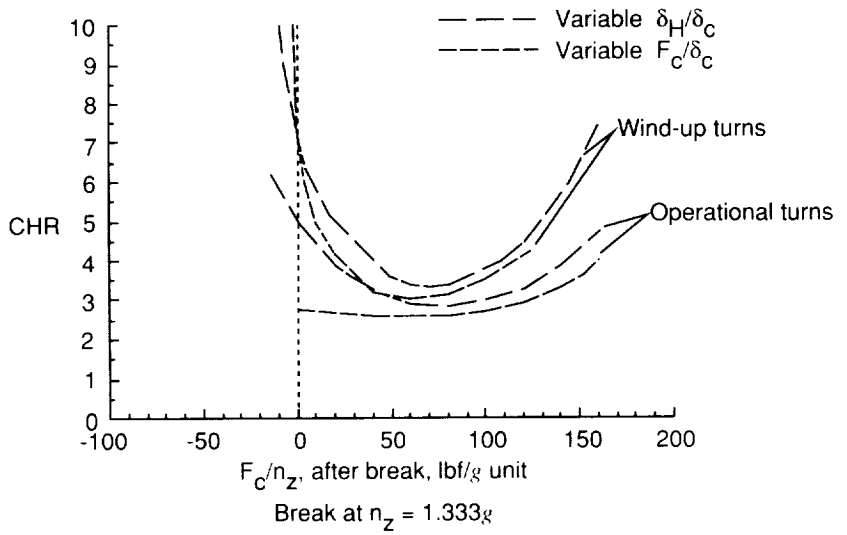

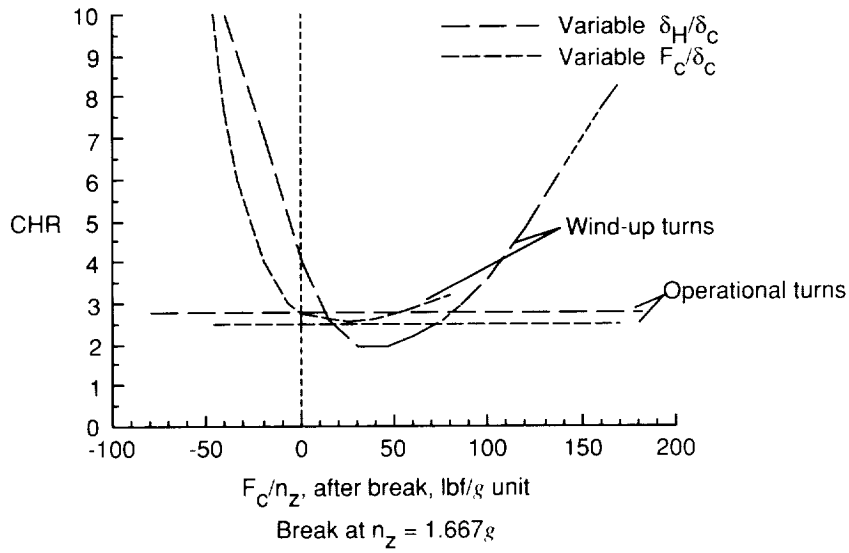

(a) c.g. = 0.40$\bar{c}$; SM = 5 percent.

Figure 27. Comparison of pilot rating trends of individual tasks with single break in maneuver stability curves. Initial slope = 50 lbf/g.

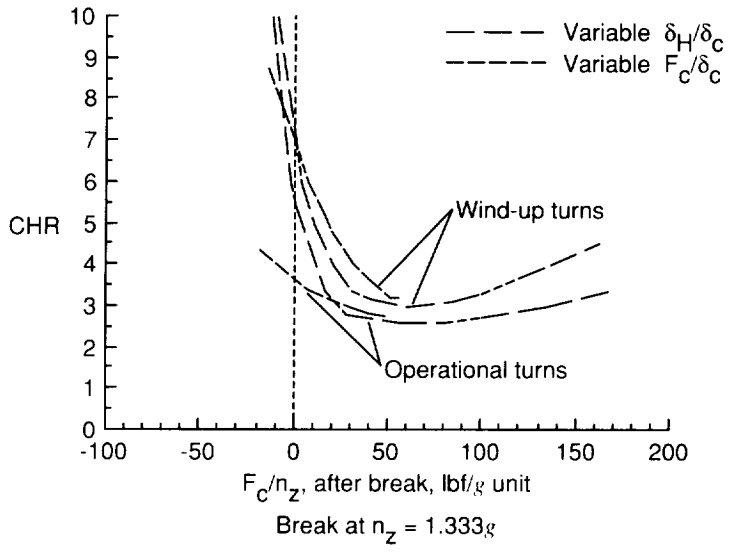

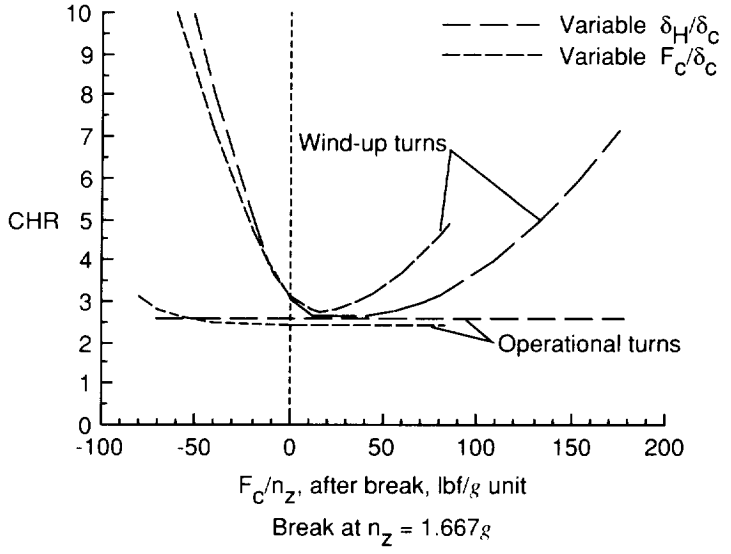

(b) c.g. = 0.50$\bar{c}$; SM = −5 percent.

Figure 27. Concluded.

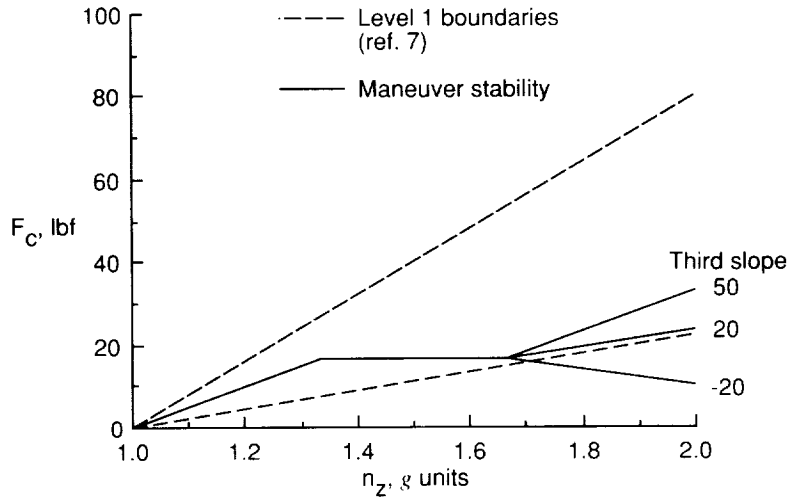

(a) Second slope of zero.

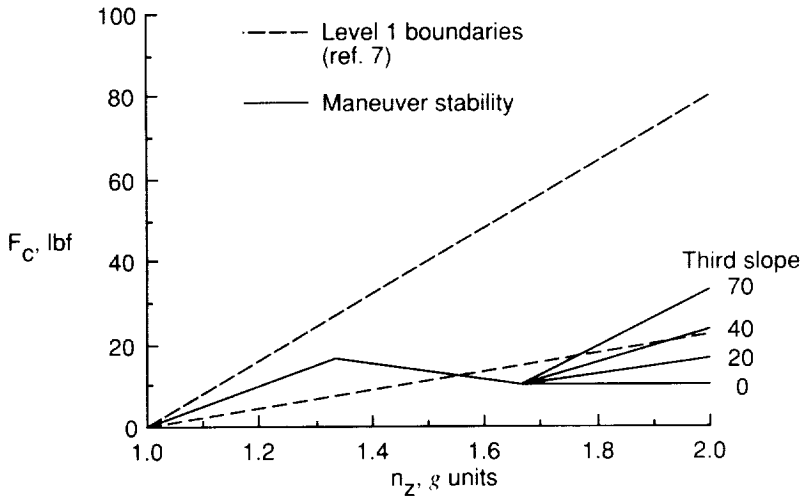

(b) Second slope of -20 lbf/g.

Figure 28. Configurations 152 through 170 with double break in maneuver curves. Initial slope = 50 lbf/g.

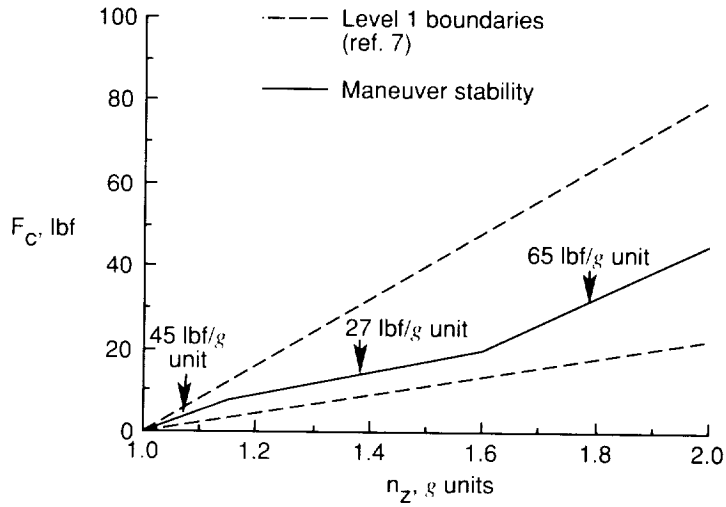

Figure 29. Preferred maneuver stability characteristics of the test airplane by pilot number one.